mathematics

MDPI

Article

Closed-Form Solutions in a Magneto-Electro-Elastic Circular Rod via Generalized Exp-Function Method

Muhammad Shakeel [1,†], Attaullah [1], Mohammed Kbiri Alaoui [2], Ahmed M. Zidan [2], Nehad Ali Shah [3,†] and Wajaree Weera [4,*]

[1] Department of Mathematics, University of Wah, Wah Cantt 47040, Pakistan
[2] Department of Mathematics, College of Science, King Khalid University, P.O. Box 9004, Abha 61413, Saudi Arabia
[3] Department of Mechanical Engineering, Sejong University, Seoul 05006, Korea
[4] Department of Mathematics, Faculty of Science, Khon Kaen University, Khon Kaen 40002, Thailand
* Correspondence: author wajawe@kku.ac.th
† These authors contributed equally to this work and are co-first authors.

Abstract: In this study, the dispersal caused by the transverse Poisson's effect in a magneto-electro-elastic (MEE) circular rod is taken into consideration using the nonlinear longitudinal wave equation (LWE), a mathematical physics problem. Using the generalized exp-function method, we investigate the families of solitary wave solutions of one-dimensional nonlinear LWE. Using the computer program Wolfram Mathematica 10, these new exact and solitary wave solutions of the LWE are derived as trigonometric function, periodic solitary wave, rational function, hyperbolic function, bright and dark solitons solutions, sinh, cosh, and sech^2 function solutions of the LWE. These solutions represent the electrostatic potential and pressure for LWE as well as the graphical representation of electrostatic potential and pressure.

Keywords: generalized exp $(-\varphi(\eta))$ expansion method; exact solutions; new optical solitons; nonlinear longitudinal wave equation

MSC: 83C15; 35A20; 35C05; 35C07; 35C08

check for updates

Citation: Shakeel, M.; Attaullah; Kbiri Alaoui, M.; Zidan, A.M.; Shah, N.A.; Weera, W. Closed-Form Solutions in a Magneto-Electro-Elastic Circular Rod via Generalized Exp-Function Method. *Mathematics* **2022**, *10*, 3400. https://doi.org/10.3390/math10183400

Academic Editor: Vasily Novozhilov

Received: 10 August 2022
Accepted: 15 September 2022
Published: 19 September 2022

Publisher's Note: MDPI stays neutral with regard to jurisdictional claims in published maps and institutional affiliations.

Copyright: © 2022 by the authors. Licensee MDPI, Basel, Switzerland. This article is an open access article distributed under the terms and conditions of the Creative Commons Attribution (CC BY) license (https://creativecommons.org/licenses/by/4.0/).

1. Introduction

A travelling wave pulse known as a soliton is the result of specific nonlinear partial differential equations. Due to its exceptional stability characteristics, this particular wave may be used in numerous significant applications [1]. In particular, solitary waves reemerge after complete nonlinear interaction, maintaining their identities with virtually the same speed and form, while most dispersive waves disperse inelastically and lose "energy" due to radiation. For instance, the wave-breaking phenomenon and formation of an optical shock are frequently associated with the propagation of a strong laser beam through an optical crystal or fiber. This phenomenon is crucial to the movement of light pulses through fiber optic systems used for digital communication [2].

The nonlinear interaction of ultrafast optical pulses with periodic media is now important from a practical standpoint. This is because researchers are looking for novel pulse propagation features with potentially very useful applications. In the middle of the 1980s, experiments on pulse propagation via periodic resonantly absorbing media started, and they are still ongoing today. The kinetics of pulse propagation in Bragg gratings under various circumstances was the subject of additional research. The formation of solitons in the presence of a weak violation of the Bragg conditions, investigations of oscillating soliton-like solutions affected by inhomogeneous broadening spectra of two-level atoms, and the delay of pulse reflection from Bragg gratings were of particular interest to researchers. Theoretical predictions of the formation of an optical zumeron and oscillating gap 2π pulses

in resonantly absorbing lattices should also be mentioned. In his monograph, Mantsyzov reviewed the findings of his research as well as a multitude of literature on the issue of periodic media's optics. The one-parameter solitons subfamily is found in [3], where the solution is stated at the band-gap edge in a sech-like form. Asymptotically reducing the equation system to the nonlinear Schrodinger equation is an alternate strategy for locating an analytical soliton-like solution. By including phase modulation into the zero-velocity solitons during numerical simulation, steady-moving solitons were produced [4].

The Scottish engineer John Russell tracked a single water wave for the first time in 1834 as it went two miles down a canal without exhibiting any discernible deformation from dispersion [5]. Wave propagation in magneto-electro-elastic (MEE) media has drawn the attention of many academics due to the growing use of MEE structures in a variety of engineering domains (such as sensors, actuators, etc.) Chen et al. [6] offered an analytical treatment for the propagation of harmonic waves in MEE multilayered plates using the propagator matrix and state-vector techniques. When axial shear MEE waves propagate in piezoelectric-piezomagnetic composites, Chen and Shen [7] found the effective wave velocity and attenuation factor. For the propagation of harmonic waves in inhomogeneous (functionally graded) MEE plates, Wu et al. [8] developed a dynamic solution.

Many researchers discovered the solitary wave solutions of various nonlinear partial differential equations, such as Seadawy [9,10], who used mathematical techniques to find the electrostatic potential and pressure for the nonlinear higher-order Kadomtsev–Petviashvili dynamical equation in two dimensions and the electric field potential, quantum statistical pressure, and electric and magnetic field. The nonlinear three-dimensional Zakharov–Kuznetsov–Burgers equation has a single wave solution that takes the form of electric and magnetic fields potential and pressure, according to Abdullah et al. [11].

For better information, to understand the mechanism and its applications, it is crucial to examine exact travelling and solitary wave solutions of nonlinear evolution equations. As a result, several scholars present novel techniques to examine the solutions of these nonlinear partial differential equations. The homogeneous balance method [12], the exp-function method [13], the tanh and extended-function method [14,15], the extended direct algebraic method [16], the modified simple equation method [17], the (G'/G)-expansion method [18,19], the modified extended tanh function method [20], the iteration transform method [21,22], and homotopy perturbation method [23] are a few examples of important methods. Using these techniques, numerous researchers have discovered various kinds of exact and solitary wave solutions to various nonlinear evolution equations, for example, see references [24–32]. It is reminiscent of Lie algebraic methods, another class of strong algebraic techniques that are frequently employed to solve nonlinear ordinary differential equations [33–35].

The generalized exp-function method is regarded being one of the most powerful techniques for solving nonlinear differential equations. Numerous studies show that this method performs exceptionally well when dealing with nonlinear differential equations. For example, Shakeel et al. [36] found novel closed-form solutions in the form of hyperbolic, trigonometric, and rational function solutions by using the generalized exp-function method for nonlinear dispersive modified Benjamin–Bona–Mahony equations. In nonlinear optics, Yahya et al. [37] demonstrated the suitability of the generalized exp $(-\phi(\eta))$ expansion method for solving nonlinear Korteweg–de Vries equation and the modified Zakharov–Kuznetsov equation. The generalized exp $(-\phi(\eta))$ expansion method is used in this paper to find an amount of new optical solitons for the nonlinear longitudinal wave equation in a magneto-electro-elastic circular rod.

The exp $(-\phi(\eta))$ expansion method is effective for solving NPDEs and can lead to numerous previously unknown closed-form solutions. The goal of this work is to generate many new and more general closed-form solutions. To that end, we propose a novel generalized approach to investigate NLEEs based on the exp $(-\phi(\eta))$ expansion method. To demonstrate the effectiveness and benefits of this method, we apply it to the nonlinear

longitudinal wave equation. A comparison of the obtained solutions is also given in the form of Table 1.

Table 1. Comparison of Solutions.

Our Solutions	Baskonus et al. [38]
If we put in $A_1 = 1, A_2 = 0, A_3 = 0, A_4 = 1, k_1 = 1, k_2 = -1, \eta = \zeta, E = c_1, N = 1, c = 2$, and $U_1(z,t) = u_5(x,t)$ in Equation (52), then $u_5(x,t) = 3 + \frac{2\sqrt{-3}}{\tanh\frac{1}{2}\sqrt{-3}((\zeta+c_1)+1)} - \frac{4}{\tanh\frac{1}{2}\sqrt{-3}((\zeta+c_1)+1)^2}$.	If we put $n = -1, r = 2, c = 1, k = 1$, and $\mu = 1$ in Equation (30), then $u_5(x,t) = 3 + \frac{2\sqrt{-3}}{\tanh\frac{1}{2}\sqrt{-3}((\zeta+c_1)+1)} - \frac{4}{\tanh\frac{1}{2}\sqrt{-3}((\zeta+c_1)+1)^2}$.
If we put in $A_1 = 1, A_2 = 0, A_3 = 0, A_4 = 1, k_1 = 1, k_2 = -1, \eta = \zeta, E = c_1, N = 1, c = 2$, and $U_4(z,t) = u_3(x,t)$ in Equation (55), then $u_3(x,t) = \frac{3}{2} + \frac{2\sqrt{-3}}{\tanh\frac{1}{2}\sqrt{-3}((\zeta+c_1)-1)} - \frac{4}{\tanh\frac{1}{2}\sqrt{-3}((\zeta+c_1)-1)^2}$.	If we put $n = -1, r = 2, c = 1, k = 1, \lambda = 1$, and $\mu = 1$ in Equation (28), then $u_3(x,t) = \frac{3}{2} + \frac{2\sqrt{-3}}{\tanh\frac{1}{2}\sqrt{-3}((\zeta+c_1)-1)} - \frac{4}{\tanh\frac{1}{2}\sqrt{-3}((\zeta+c_1)-1)^2}$.
If we put in $A_1 = 1, A_2 = 0, A_3 = 0, A_4 = 1, k_1 = 1, k_2 = -1, \eta = \zeta, E = c_1, N = 1, c = 2$, and $U_7(z,t) = u_1(x,t)$ in Equation (58), then $u_1(x,t) = 3 - \frac{2\sqrt{21}}{\tanh\frac{1}{2}\sqrt{3}\left((\eta+E)-\sqrt{7}\right)} + \frac{4}{\tanh\frac{1}{2}\sqrt{3}\left((\eta+E)-\sqrt{7}\right)^2}$.	If we put $n = -1, r = 2, c = 1, k = 1$, and $\mu = 1$ in Equation (26), then $u_1(x,t) = 3 - \frac{2\sqrt{21}}{\tanh\frac{1}{2}\sqrt{3}\left((\eta+E)-\sqrt{7}\right)} + \frac{4}{\tanh\frac{1}{2}\sqrt{3}\left((\eta+E)-\sqrt{7}\right)^2}$.

The structure of this article is as follows. We go over the fundamental equations for MEE materials in Section 2. The longitudinal wave equations for a MEE circular rod are determined in Section 3. In Section 4, the general procedure of the proposed method is given. Section 5 consists of the application of the proposed method to find the solitary wave solutions. Results and discussion are provided in Section 6, and conclusion is given in Section 7.

2. Fundamental Equations

Assumedly, the rod is formed of a transversely isotropic MEE material with a z-axis of symmetry (i.e., the rod direction). Consequently, the fundamental relationships in it make it possible to write the cylindrical coordinate system (r, θ, z) as

$$\begin{cases} \rho_r = c_{11}\varepsilon_r + c_{12}\varepsilon_\theta + c_{13}\varepsilon_z - e_{31}E_z - q_{31}H_z, \\ \rho_\theta = c_{12}\varepsilon_r + c_{11}\varepsilon_\theta + c_{13}\varepsilon_z - e_{31}E_z - q_{31}H_z, \\ \rho_z = c_{13}\varepsilon_r + c_{13}\varepsilon_\theta + c_{33}\varepsilon_z - e_{33}E_z - q_{33}H_z, \\ \psi_{rz} = c_{44}\phi_{rz} - e_{15}E_r - q_{15}H_r, \\ \psi_{\theta z} = c_{44}\phi_{\theta z} - e_{15}E_\theta - q_{15}H_\theta, \\ \psi_{r\theta} = c_{66}\phi_{r\theta}, \end{cases} \tag{1}$$

$$\begin{cases} \alpha_r = e_{15}\phi_{rz} + \varepsilon_{11}E_r + d_{11}H_r, \\ \alpha_\theta = e_{15}\phi_{rz} + \varepsilon_{11}E_r + d_{11}H_r, \\ \alpha_z = e_{31}\varepsilon_r + e_{31}\varepsilon_\theta + e_{33}\varepsilon_z + \varepsilon_{33}E_z + d_{33}H_z, \end{cases} \tag{2}$$

$$\begin{cases} P_r = q_{15}\phi_{rz} + d_{11}E_r + \varpi_{11}H_r, \\ P_\theta = q_{15}\phi_{\theta z} + d_{11}E_\theta + \varpi_{11}H_\theta, \\ P_z = q_{31}\varepsilon_r + q_{31}\varepsilon_\theta + q_{33}\varepsilon_z + d_{33}E_z + \varpi_{33}H_z, \end{cases} \tag{3}$$

where the normal and shear stresses are ρ_i and ψ_{ij}, and the normal and shear strains are ε_i and ϕ_{ij}; the electric field, magnetic field, electric displacement, and magnetic induction are denoted by the letters E_i, H_i, α_i, and P_i, respectively. The elastic, dielectric, piezoelectric, magneto-electric, and magnetic coefficients are denoted by the letters c_{ij}, ε_{ij}, e_{ij}, q_{ij}, d_{ij}, and ϖ_{ij}, respectively. It should be noticed that the relationship $c_{11} = c_{12} + 2c_{66}$ holds for the transversely isotropic material.

Additionally, the equations of motion for the rod are as follows in the absence of body forces, electric charges, and magnetic charges:

$$\begin{cases} \beta\frac{\partial^2 U_r}{\partial t^2} = \frac{\partial \rho_r}{\partial r} + \frac{\partial \psi_{r\theta}}{r\partial\theta} + \frac{\partial \psi_{rz}}{\partial z} + \frac{\rho_r - \rho_\theta}{r}, \\ \beta\frac{\partial^2 U_\theta}{\partial t^2} = \frac{\partial \psi_{r\theta}}{\partial r} + \frac{\partial \rho_\theta}{r\partial\theta} + \frac{\partial \psi_{\theta z}}{\partial z} + 2\frac{\psi_{r\theta}}{r}, \\ \beta\frac{\partial^2 U_z}{\partial t^2} = \frac{\partial \psi_{rz}}{\partial r} + \frac{\partial \psi_{\theta z}}{r\partial\theta} + \frac{\partial \rho_r}{\partial z} + \frac{\psi_{rz}}{r}, \end{cases} \tag{4}$$

$$\frac{\partial \alpha_r}{\partial r} + \frac{\partial \alpha_\theta}{r\partial\theta} + \frac{\partial \alpha_z}{\partial z} = 0, \tag{5}$$

$$\frac{\partial P_r}{\partial r} + \frac{\partial P_\theta}{r\partial\theta} + \frac{\partial P_z}{\partial z} = 0, \tag{6}$$

where the mechanical displacements in the $r-$, $\theta-$, and $z-$ directions are represented by U_r, U_θ, and U_z, respectively.

The electric field-potential, magnetic field-potential, and finite (nonlinear) elastic strain-displacement relationships can be described as

$$E_r = -\frac{\partial \varphi}{\partial r}, \quad E_\theta = -\frac{\partial \varphi}{r\partial\theta}, \quad E_z = -\frac{\partial \varphi}{\partial z}, \tag{7}$$

$$H_r = -\frac{\partial \zeta}{\partial r}, \quad H_\theta = -\frac{\partial \zeta}{r\partial\theta}, \quad H_z = -\frac{\partial \zeta}{\partial z}, \tag{8}$$

$$\begin{cases} \varepsilon_r = \frac{\partial U_r}{\partial r}, \quad \varepsilon_\theta = \frac{\partial U_\theta}{r\partial\theta} + \frac{U_r}{r}, \quad \varepsilon_z = \frac{\partial U_z}{\partial z} + \frac{1}{2}\left(\frac{\partial U_z}{\partial z}\right)^2, \\ \hbar_{r\theta} = \frac{\partial U_r}{r\partial\theta} + \frac{\partial U_\theta}{\partial r} - \frac{U_\theta}{r}, \ \hbar_{\theta z} = \frac{\partial U_z}{r\partial\theta} + \frac{\partial U_\theta}{\partial z}, \ \hbar_{rz} = \frac{\partial U_z}{\partial r} + \frac{\partial U_r}{\partial z} \end{cases} \tag{9}$$

where the electric potential is φ, and the magnetic potential is ζ, respectively. It should be noted that we made the assumption that the normal strain component in the longitudinal rod direction (z-direction) is finite while formulating Equation (9).

3. Longitudinal Wave Equations in a MEE Circular Rod

As depicted in Figure 1, we take into account wave propagation in a long MEE circular rod. Z is along the rod direction, or the direction in which waves propagate, in the cylindrical coordinate system (r, θ, z), and $\theta \in [0,\ 2\pi]$, $0 \le r \le R$. The following assumptions are made to aid our study:

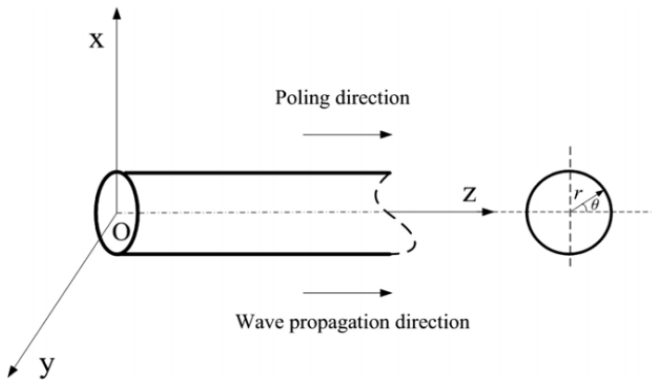

Figure 1. Shows a schematic for a long, circular MEE rod [2].

(i) The rod's cross-section remains plain both before and after the deformation;

(ii) The rod's lateral surface has axial symmetry, suggesting that $U_\theta = 0$ and $\partial/\partial\theta = 0$;

(iii) To take into account the Poisson's effect, the radial displacement U_r and the gradient of the longitudinal displacement U_z are linked by $U_r = -v_{eff}\, r\partial U_z/\partial z$, where v_{eff} is the effective Poisson's ratio that will be computed later.

Additionally, because the problem is one-dimensional, there should be zero extended tractions on the rod's lateral boundary. In other words, the following relations are established from the equations: $\rho_r = 0$, $\psi_{rz} = 0$, $\psi_{r\theta} = 0$, $\alpha_r = 0$, and $P_r = 0$:

$$\begin{cases} \hbar_{rz} = \hbar_{\theta z} = 0, E_r = E_\theta = 0, \\ H_r = H_\theta = 0, \alpha_\theta = P_\theta = 0, \end{cases} \tag{10}$$

$$\varepsilon_r = \frac{e_{31}E_z + q_{31}H_z - c_{12}\varepsilon_\theta - c_{13}\varepsilon_z}{c_{11}}. \tag{11}$$

The equations of motion are reduced to the following forms when we allow $U = U_z$ to represent the longitudinal displacement.

$$\frac{-\rho_r}{r} = \beta\frac{\partial^2 U_r}{\partial t^2}, \ \frac{\partial \rho_z}{\partial z} = \beta\frac{\partial^2 U}{\partial t^2}, \tag{12a}$$

$$\frac{\partial \alpha_z}{\partial z} = 0, \tag{12b}$$

$$\frac{\partial P_z}{\partial z} = 0. \tag{12c}$$

In terms of U, φ, and ψ, these equations become

$$v_{eff}\beta r^2\frac{\partial^3 U}{\partial t^2 \partial z} = F_1\frac{\partial \varphi}{\partial z} + F_2\frac{\partial \zeta}{\partial z} - F_3 v_{eff}\frac{\partial U}{\partial z} + F_4\varepsilon_z, \tag{13}$$

$$\beta\frac{\partial^2 U}{\partial t^2} = \frac{\partial}{\partial z}\left[B_1\frac{\partial \varphi}{\partial z} + B_2\frac{\partial \zeta}{\partial z} - F_4 v_{eff}\frac{\partial U}{\partial z} + B_4\varepsilon_z\right], \tag{14}$$

$$\frac{\partial}{\partial z}\left[C_1\frac{\partial \varphi}{\partial z} + C_2\frac{\partial \zeta}{\partial z} + F_1 v_{eff}\frac{\partial U}{\partial z} - B_1\varepsilon_z\right] = 0, \tag{15}$$

$$\frac{\partial}{\partial z}\left[C_2\frac{\partial \varphi}{\partial z} + D_2\frac{\partial \zeta}{\partial z} + F_2 v_{eff}\frac{\partial U}{\partial z} - B_2\varepsilon_z\right] = 0, \tag{16}$$

where

$$\left\{F_1 = e_{31}\left(1 - \frac{c_{12}}{c_{11}}\right), \ F_2 = q_{31}\left(1 - \frac{c_{12}}{c_{11}}\right), \ F_3 = c_{11} - \frac{c^2{}_{12}}{c_{11}}, \ F_4 = c_{13}\left(1 - \frac{c_{12}}{c_{11}}\right), \right. \tag{17a}$$

$$\left\{B_1 = e_{33} - \frac{c_{13}}{c_{11}}e_{31}, \ B_2 = q_{33} - \frac{c_{13}}{c_{11}}q_{31}, \ B_4 = c_{33} - \frac{c^2{}_{13}}{c_{11}}, \right. \tag{17b}$$

$$\left\{C_1 = \varepsilon_{33} + \frac{e_{31}}{c_{11}}e_{31}, \ C_2 = d_{33} + \frac{e_{31}}{c_{11}}q_{31}, \ D_2 = \varpi_{33} + \frac{q_{31}}{c_{11}}q_{31}. \right. \tag{17c}$$

Differentiating Equation (13) with respect to z, we obtain

$$\beta v_{eff} r^2\frac{\partial^4 U}{\partial t^2 \partial z^2} = F_1\frac{\partial^2 \varphi}{\partial z^2} + F_2\frac{\partial^2 \zeta}{\partial z^2} - F_3 v_{eff}\frac{\partial^2 U}{\partial z^2} + F_4\frac{\partial \varepsilon_z}{\partial z}, \tag{18}$$

Integrating Equation (18) over the cross section of the rod, we arrive at

$$-F_4\frac{\partial \varepsilon_z}{\partial z} + \frac{1}{2}\beta v_{eff} R^2\frac{\partial^4 U}{\partial t^2 \partial z^2} = F_1\frac{\partial^2 \varphi}{\partial z^2} + F_2\frac{\partial^2 \zeta}{\partial z^2} - F_3 v_{eff}\frac{\partial^2 U}{\partial z^2}. \tag{19}$$

Now, we solve Equations (15), (16), and (19) to find the values of φ, ζ, and U as

$$\frac{\partial^2 \varphi}{\partial z^2} = \frac{\Omega_1}{\Omega}, \ \frac{\partial^2 \zeta}{\partial z^2} = \frac{\Omega_2}{\Omega}, \ \frac{\partial^2 U}{\partial z^2} = \frac{\Omega_3}{\Omega}, \tag{20}$$

where

$$\Omega = \begin{vmatrix} F_1 & F_2 & -v_{eff}F_3 \\ C_1 & C_2 & v_{eff}F_1 \\ C_2 & D_2 & v_{eff}F_2 \end{vmatrix}, \tag{21a}$$

$$\Omega_1 = \begin{vmatrix} \frac{1}{2}\beta v_{eff}R^2\frac{\partial^4 U}{\partial t^2\partial z^2} - F_4\frac{\partial \varepsilon_z}{\partial z} & F_2 & -v_{eff}F_3 \\ B_1\frac{\partial \varepsilon_z}{\partial z} & C_2 & v_{eff}F_1 \\ B_2\frac{\partial \varepsilon_z}{\partial z} & D_2 & v_{eff}F_2 \end{vmatrix}, \tag{21b}$$

$$\Omega_2 = \begin{vmatrix} F_1 & \frac{1}{2}\beta v_{eff}R^2\frac{\partial^4 U}{\partial t^2\partial z^2} - F_4\frac{\partial \varepsilon_z}{\partial z} & -v_{eff}F_3 \\ C_1 & B_1\frac{\partial \varepsilon_z}{\partial z} & v_{eff}F_1 \\ C_2 & B_2\frac{\partial \varepsilon_z}{\partial z} & v_{eff}F_2 \end{vmatrix}, \tag{21c}$$

$$\Omega_3 = \begin{vmatrix} F_1 & F_2 & \frac{1}{2}\beta v_{eff}R^2\frac{\partial^4 U}{\partial t^2\partial z^2} - F_4\frac{\partial \varepsilon_z}{\partial z} \\ C_1 & C_2 & B_1\frac{\partial \varepsilon_z}{\partial z} \\ C_2 & D_2 & B_2\frac{\partial \varepsilon_z}{\partial z} \end{vmatrix}. \tag{21d}$$

Equation (20) is substituted into Equation (14) to obtain

$$\beta\frac{\partial^2 U}{\partial t^2} - B_4\frac{\partial \varepsilon_z}{\partial z} = \frac{1}{\Omega}\Big(B_1\Omega_1 + B_2\Omega_2 - v_{eff}A_4\Omega_3\Big). \tag{22}$$

The longitudinal wave equation for a MEE circular rod is obtained by taking derivative of Equation (22) with respect to z and using the finite elastic strain-displacement relation from Equation (9):

$$\beta\frac{\partial^2 u}{\partial t^2} - B_4\frac{\partial^2}{\partial z^2}\left(u + \frac{u^2}{2}\right) = \frac{1}{\Omega}\Big(B_1\Omega_1^* + B_2\Omega_2^* - v_{eff}F_4\Omega_3^*\Big), \tag{23}$$

where

$$u = \partial U/\partial z, \text{ and}$$

$$\begin{aligned}\Omega_1^* = \; & v_{eff}\big[-F_4(C_2F_2 - F_1D_2) - B_1\big(F_2^2 + F_3D_2\big) + B_2(F_1F_2 + C_2F_3)\big]\tfrac{\partial^2}{\partial z^2}\big(u + u^2/2\big) \\ & + \tfrac{\beta}{2}v_{eff}^2R^2(C_2F_2 - F_1D_2)\,\tfrac{\partial^4 u}{\partial t^2\partial z^2},\end{aligned} \tag{24a}$$

$$\begin{aligned}\Omega_2^* = \; & v_{eff}\big[A_4(C_1F_2 - F_1C_2) + B_1(F_1F_2 + F_3C_2) - B_2\big(F_1^2 + C_1F_3\big)\big]\tfrac{\partial^2}{\partial z^2}\big(u + u^2/2\big) \\ & - \tfrac{\beta}{2}v_{eff}^2R^2(C_1F_2 - F_1C_2)\,\tfrac{\partial^4 u}{\partial t^2\partial z^2},\end{aligned} \tag{24b}$$

$$\begin{aligned}\Omega_3^* = \; & \big[-F_4\big(C_1D_2 - C_2^2\big) - B_1(F_1D_2 - C_2F_2) + B_2(F_1C_2 - C_1F_2)\big]\tfrac{\partial^2}{\partial z^2}\big(u + u^2/2\big) \\ & + \tfrac{\beta}{2}v_{eff}R^2\big(C_1D_2 - C_2^2\big)\,\tfrac{\partial^4 u}{\partial t^2\partial z^2},\end{aligned} \tag{24c}$$

Equation (23) can also be transformed into the normative nonlinear wave equation shown below:

$$\frac{\partial^2 u}{\partial\, t^2} - c_0^2\frac{\partial^2 u}{\partial\, z^2} = \frac{\partial^2}{\partial\, z^2}\left(\frac{1}{2}c_0^2u^2 + N\frac{\partial^2 u}{\partial\, t^2}\right), \tag{25}$$

with

$$\begin{aligned}c_0^2 = \; & \tfrac{v_{eff}}{\Omega\beta}\big[B_1\big\{-F_4(C_2F_2 - F_1D_2) - B_1(F_2^2 + F_3D_2) + B_2(F_1F_2 + C_2F_3)\big\} \\ & + B_2\big\{F_4(C_1F_2 - F_1C_2) + B_1(F_1F_2 + F_3C_2) - B_2(F_1^2 + C_1F_3)\big\} \\ & - F_4\big\{-F_4(C_1D_2 - C_2^2) - B_1(F_1D_2 - C_2F_2) + B_2(F_1C_2 - C_1F_2)\big\}\big] + \tfrac{B_4}{\beta},\end{aligned} \tag{26}$$

$$\begin{aligned}N = \; & \tfrac{v_{eff}}{2}R^2[B_1(C_2F_2 - F_1D_2) - B_2(C_1F_2 - F_1C_2) - F_4(C_1D_2 - C_2^2)] \\ & [F_1(C_2F_2 - F_1D_2) - F_2(C_1F_2 - F_1C_2) - F_3(C_1D_2 - C_2^2)]^{-1},\end{aligned} \tag{27}$$

where N is the dispersion parameter, and c_0 is the linear longitudinal wave velocity for a MEE circular rod, both of which rely on the characteristics of the material and the rod's geometry.

If we cogitate as $c_0 = c$ for simplicity, we can rewrite Equation (25) as

$$\frac{\partial^2 u}{\partial t^2} - c^2 \frac{\partial^2 u}{\partial z^2} = \frac{\partial^2}{\partial z^2}\left(\frac{1}{2}c^2 u^2 + N\frac{\partial^2 u}{\partial t^2}\right). \tag{28}$$

Wave propagation in magneto-electroelastic (MEE) media has been studied by numerous researchers as a result of the expanding applications of MEE structures in various engineering domains (such as actuators, sensors, etc.) over time [5–7,39]. Using a modified exp(-Ω(ξ))-expansion function approach, Baskonus et al. [38] identified the hyperbolic function and complex hyperbolic function solutions of the nonlinear longitudinal wave equation (LWE) in a MEE circular rod. In their study of numerical solitary wave solutions, Xue et al. [2] used the dispersion caused by the transverse Poisson's effect in a MEE circular rod to derive the nonlinear LWE. The ansatz, modified (G'/G)-expansion, and functional variable techniques are just a few of the innovative analytical solutions of the LWE in a MEE circular rod that have been researched [39–41]. Recently, Seadawy [42] used the extended trial equation method to find the soliton and other types of solutions of nonlinear LWE in a MEE circular rod. The combination of piezoelectric $BaTiO_3$ and piezomagnetic $CoFe_2O_4$ with various values of the volume fraction (v_f) of piezoelectric $BaTiO_3$ is the bodily meaning of nonlinear LWE in MEE circular rod. The rod's radius is given as r = 0.05 m.

4. The Generalized Exp-Function Method

Assume we have a nonlinear PDE given below of the form

$$F\left(U,\ U_z,\ U_t,\ U_{zz},\ U_{tt},\ U_{zt},\ U_{zzt},\ldots\right) = 0, \tag{29}$$

in which U is an unidentified function, and F is a polynomial in U and its derivatives with respect to z and t, including highest-order derivatives and non-linear terms. The following are the major steps in the generalized exp-function method:

Step 1. The travelling wave transformation

$$U(z,t) = u(\eta),\quad \eta = k_1 z + k_2 t, \tag{30}$$

where k_1 and k_2 are unknown constants, transforming Equation (29) into an ordinary differential equation (ODE).

$$P\left(u,\ k_1 u',\ k_2 u',\ k_1 k_2 u'',\ldots\right) = 0. \tag{31}$$

Step 2. Suppose the trial solution of Equation (31) is as follows:

$$u(\eta) = \sum_{i=0}^{m} a_i \left[\exp\left(-\frac{A_1\,\varphi(\eta) + A_2}{A_3\,\varphi(\eta) + A_4}\right)\right]^i, \tag{32}$$

where a_i, $a_m \neq 0$, $(0 \leq i \leq m)$ are undefined constants, and $\phi(\eta)$ satisfies the differential equation:

$$\phi'(\eta) = \frac{(A_3\,\phi(\eta) + A_4)^2}{(A_1 A_4 + A_2 A_3)}\left(\exp\left(-\frac{A_1\,\phi(\eta) + A_2}{A_3\,\phi(\eta) + A_4}\right) + A\exp\left(\frac{A_1\,\phi(\eta) + A_2}{A_3\,\phi(\eta) + A_4}\right) + B\right), \tag{33}$$

where $\Delta = (A_1 A_4 - A_2 A_3) \neq 0$. Equation (33) has the following solution families:

Family 1. When $\Delta = (A_1 A_4 - A_2 A_3) \neq 0$, $A \neq 0$, $\left(B^2 - 4A\right) > 0, A_2 = 0$,

$$\phi_1(\eta) = \frac{A_4 \ln\left(\left(-\sqrt{B^2-4A}\tanh\left(\frac{\sqrt{B^2-4A}}{2}(\eta+E)\right)-B\right)/2A\right)}{A_1 - A_3 \ln\left(\left(-\sqrt{B^2-4A}\tanh\left(\frac{\sqrt{B^2-4A}}{2}(\eta+E)\right)-B\right)/2A\right)}. \quad (34)$$

Family 2. When $\Delta = (A_1 A_4 - A_2 A_3) \neq 0$, $A \neq 0$, $\left(B^2 - 4A\right) < 0$, $A_2 = 0$,

$$\phi_2(\eta) = \frac{A_4 \ln\left(\left(\sqrt{-B^2+4A}\tan\left(\frac{\sqrt{-B^2+4A}}{2}(\eta+E)\right)-B\right)/2A\right)}{A_1 - A_3 \ln\left(\left(\sqrt{-B^2+4A}\tan\left(\frac{\sqrt{-B^2+4A}}{2}(\eta+E)\right)-B\right)/2A\right)}. \quad (35)$$

Family 3. When $\Delta = (A_1 A_4 - A_2 A_3) \neq 0$, $A \neq 0, B \neq 0$, $\left(B^2 - 4A\right) = 0$, $A_2 = 0$,

$$\phi_3(\eta) = \frac{A_4 \ln\left(-\left(2(B(\eta+E))+2\right)/B^2(\eta+E)\right)}{A_1 - A_3 \ln(-2\left(B(\eta+E)\right)+2)/B^2(\eta+E)}. \quad (36)$$

Family 4. When $\Delta = (A_1 A_4 - A_2 A_3) \neq 0$, $A \neq 0, B \neq 0$, $\left(B^2 - 4A\right) > 0$, $A_3 = 0$,

$$\phi_4(\eta) = -2(A_2/A_1) + (A_4/A_1)\ln(-\tanh\left(\sqrt{(B^2-4A)}\frac{(\eta+E)}{2}\right)\sqrt{e^{(\frac{2A_2}{A4})}(B^2-4A)} - Be^{(\frac{A_2}{A_4})}/2A). \quad (37)$$

Family 5. When $\Delta = (A_1 A_4 - A_2 A_3) \neq 0$, $B \neq 0$, $A \neq 0$, $\left(B^2 - 4A\right) < 0$, $A_3 = 0$,

$$\phi_5(\eta) = -2(A_2/A_1) + (A_4/A_1)\ln(-\tan\left(\sqrt{(-B^2+4A)}\frac{(\eta+E)}{2}\right)\sqrt{e^{(\frac{2A_2}{A4})}(-B^2+4A)} - Be^{(\frac{A_2}{A_4})}/2A). \quad (38)$$

Family 6. When $\Delta = (A_1 A_4 - A_2 A_3) \neq 0$, $A \neq 0, B \neq 0$, $\left(B^2 - 4A\right) = 0$, $A_3 = 0$,

$$\phi_6(\eta) = -(A_2/A_1) + (A_4/A_1)\ln((2(B(\eta+E)+2))/B^2(\eta+E)). \quad (39)$$

Family 7. When $\Delta = (A_1 A_4 - A_2 A_3) \neq 0$, $A = 0, B \neq 0$, $\left(B^2 - 4A\right) > 0$,

$$\phi_7(\eta) = -\frac{A_2 + A_4 \ln(B/\exp(B(\eta+E)) - 1)}{A_1 + A_3 \ln(B/\exp(B(\eta+E)) - 1)}. \quad (40)$$

Family 8. When $\Delta = (A_1 A_4 - A_2 A_3) \neq 0$, $A = 0, B = 0$, $\left(B^2 - 4A\right) = 0$,

$$\phi_8(\eta) = -\frac{A_2 - A_4 \ln(\eta+E)}{A_1 - A_3 \ln(\eta+E)}. \quad (41)$$

Family 9. When $(A_1 A_4 - A_2 A_3) \neq 0$, $A \neq 0, B \neq 0$, $\left(B^2 - 4A\right) = 0$, $A_i \neq 0$, $(i = 1, 2, 3, 4)$,

$$\phi_9(\eta) = -\frac{A_2 - A_4 \ln\left(-\frac{2(\eta+E)}{B(\eta+E)-2}\right)}{A_1 - A_3 \ln\left(-\frac{2(\eta+E)}{B(\eta+E)-2}\right)}. \quad (42)$$

Family 10. When $\Delta = (A_1 A_4 - A_2 A_3) \neq 0$, $A < 0, B = 0$,

$$\phi_{10}(\eta) = -\frac{A_2 - A_4 \ln\left(-\frac{\exp\left(-2\sqrt{-A}(\eta+E)\right)+1}{\sqrt{-A}\exp\left(-2\sqrt{-A}(\eta+E)\right)-1}\right)}{A_1 - A_3 \ln\left(-\frac{\exp\left(-2\sqrt{-A}(\eta+E)\right)+1}{\sqrt{-A}\exp\left(-2\sqrt{-A}(\eta+E)\right)-1}\right)}. \quad (43)$$

Step 3. Using the balancing principle between the highest-order derivative and the highest-order nonlinear term in Equation (31), we calculate the value of the positive integer m.

Step 4. Equation (32) is substituted into Equation (31), and then, Equation (33) is used, with all the coefficients of $\left[\exp\left(-\frac{A_1\phi(\eta)+A_2}{A_3\phi(\eta)+A_4}\right)\right]^i$ to zero, yielding an algebraic equation system for k_1, A, B, k_2 and (i = 0, 1, 2, 3, . . . , m). Solving the algebraic system of equations yields the values of the constants k_1, A, B, k_2, and a_i $(i = 0, 1, 2, \ldots, m)$ can be determined. We can substitute k_1, k_2, B, A, and a_i as well as the general solutions of Equation (33) into Equation (32) to obtain the exact solutions of nonlinear PDEs Equation (28) because we know the general solutions of Equation (33).

5. Applications

In this section, we applied the generalized exp (-$\phi(\eta)$) expansion method to the nonlinear longitudinal wave equation to obtain new closed-form solutions.

The longitudinal wave equation in a magneto-electro-elastic circular rod is transformed into a non-linear ordinary differential equation using the wave transformation Equation (30) and some mathematical operations as follows:

$$u''(\eta)k_2^2 - c^2u''(\eta)k_1^2 - c^2u(\eta)^2k_1^2 - c^2u(\eta)u''(\eta)k_1^2 - Nu^{(iv)}(\eta)k_1^2k_2^2 = 0, \tag{44}$$

where c, k_1, and k_2 are nonzero real constants.

By integrating Equation (44) twice with respect to η and taking the integral constants to be zero, we can find the following equation:

$$2Nk_1^2k_2^2u''(\eta) - 2(k_2^2 - c^2k_1^2)u(\eta) + c^2k_1^2u^2(\eta) = 0. \tag{45}$$

By applying the balancing principle between u'' and u^2 in Equation (44), we obtain $m = 2$. As a result, the trial solution Equation (32) is as follows:

$$u(\eta) = a_0 + a_1\exp\left(-\frac{A_1\phi(\eta)+A_2}{A_3\phi(\eta)+A_4}\right) + a_2\exp\left(-\frac{A_1\phi(\eta)+A_2}{A_3\phi(\eta)+A_4}\right)^2. \tag{46}$$

By inserting Equations (46) and (33) into Equation (45), we obtain a polynomial in $\left[\exp\left(-\frac{A_1\phi(\eta)+A_2}{A_3\phi(\eta)+A_4}\right)\right]^i$, $(i = 0, 1, 2, \ldots, m)$ and then equate all the coefficients of the resulting polynomial to zero, yielding a set of simultaneous algebraic equations. After solving the algebraic system with Maple 18, we obtain the following coefficient values:

Case 1.

$$\begin{aligned} a_0 &= -\frac{12NAk_2^2}{c^2}, a_1 = -\frac{12k_2\sqrt{N(4NAk_1^2k_2^2 - c^2k_1^2 + k_2^2)}}{c^2k_1}, a_2 = -\frac{12Nk_2^2}{c^2}, \\ B &= \frac{\sqrt{(4NAk_1^2k_2^2 - c^2k_1^2 + k_2^2)}}{\sqrt{N}k_1k_2}. \end{aligned} \tag{47}$$

Case 2.

$$\begin{aligned} a_0 &= -\frac{2Nk_1^2(B^2+2A)}{1+B^2Nk_1^2-4NAk_1^2}, a_1 = -\frac{2NBk_1^2}{1+B^2Nk_1^2-4NAk_1^2}, a_2 = -\frac{2Nk_1^2}{1+B^2Nk_1^2-4NAk_1^2}, \\ k_2 &= -\frac{ck_1}{\sqrt{1+B^2Nk_1^2-4NAk_1^2}}. \end{aligned} \tag{48}$$

Case 3.

$$\begin{aligned} a_0 &= -\frac{2(6NAk_1^2k_2^2 + c^2k_1^2 - k_2^2)}{c^2k_1^2}, a_1 = \frac{12k_2\sqrt{N(4NAk_1^2k_2^2 + c^2k_1^2 - k_2^2)}}{c^2k_1}, \\ a_2 &= -\frac{12Nk_2^2}{c^2}, B = -\frac{\sqrt{(4NAk_1^2k_2^2 + c^2k_1^2 - k_2^2)}}{\sqrt{N}k_1k_2}. \end{aligned} \tag{49}$$

Case 4.

$$\begin{aligned} a_0 &= a_0, a_1 = -\frac{i4k_2\sqrt{3N(c^2a_0k_1^2 + 3c^2k_1^2 - 3k_2^2)}}{c^2k_1}, a_2 = -\frac{12Nk_2^2}{c^2}, \\ A &= -\frac{c^2a_0}{12Nk_2^2}, B = -\frac{i\sqrt{c^2a_0k_1^2 + 3c^2k_1^2 - 3k_2^2}}{\sqrt{3N}k_1k_2}. \end{aligned} \tag{50}$$

Case 5.

$$\begin{aligned} a_0 &= a_0, a_1 = -\frac{i4k_2\sqrt{3N\left(c^2a_0k_1^2-c^2k_1^2+k_2^2\right)}}{c^2k_1}, a_2 = -\frac{12\,Nk_2^2}{c^2}, \\ A &= -\frac{c^2a_0k_1^2+2c^2k_1^2-2k_2^2}{12Nk_1^2k_2^2}, B = -\frac{i\sqrt{c^2a_0k_1^2-c^2k_1^2+k_2^2}}{\sqrt{3N}k_1k_2}. \end{aligned} \tag{51}$$

To begin, the hyperbolic, trigonometric, and rational function solutions to the nonlinear longitudinal wave equation are obtained by substituting the coefficient values from Equation (47) into Equation (46) and evaluating Equations (34)–(36) as follows:

$$U_1(z,t) = \frac{12A\,N^2k_2^2\left(k_2^2-c^2k_1^2\right)}{c^2\left(\alpha\,\cosh(\beta_1(k_1z+k_2t+E))+\sqrt{N\left(k_2^2-c^2k_1^2\right)}\sinh(\beta_1(k_1z+k_2t+E))\right)^2}, \tag{52}$$

where k_1, k_2, E, A, N, c are non-zero real constants and $\alpha = \sqrt{N\left(4NAk_1^2k_2^2-c^2k_1^2+k_2^2\right)}$, $\beta_1 = \frac{1}{2}\sqrt{\frac{k_2^2-c^2k_1^2}{Nk_1^2k_2^2}}$.

$$U_2(z,t) = -\frac{12A\,N^2k_2^2\left(c^2k_1^2-k_2^2\right)\,\sec^2(\beta_2\,(k_1z+k_2t+E))}{c^2\left(\sqrt{N\left(c^2k_1^2-k_2^2\right)}\,\tan\left(\beta_2\,(k_1z+k_2t+E)\right)-\alpha\right)^2}, \tag{53}$$

where k_1, k_2, E, A, N, c are non-zero real constants, and $\alpha = \sqrt{N\left(4NAk_1^2k_2^2-c^2k_1^2+k_2^2\right)}$, $\beta_2 = \frac{1}{2}\sqrt{\frac{c^2k_1^2-k_2^2}{Nk_1^2k_2^2}}$.

$$U_3(z,t) = -\frac{12\,A\,N\,k_2^2}{c^2} - \frac{6\alpha^{\frac{3}{2}}(k_1z+k_2t+E)}{k_1^2c^2(\alpha(k_1z+k_2t+E)+2Nk_1k_2)} - \frac{3N\left(4NAk_1^2k_2^2-c^2k_1^2+k_2^2\right)^2(k_1z+k_2t+E)^2}{k_1^2c^2(\alpha(k_1z+k_2t+E)+2Nk_1k_2)^2}. \tag{54}$$

where k_1, k_2, E, A, N, c are non-zero real constants, and $\alpha = \sqrt{N\left(4NAk_1^2k_2^2-c^2k_1^2+k_2^2\right)}$.

Secondly, we calculate the hyperbolic, trigonometric, and rational functions solutions for Equation (28) by substituting the coefficient values from Equation (48) into Equation (46) and considering Equations (34)–(36) as follows:

$$U_4(z,t) = -\frac{\left(H\left(B^2-6A+2KB\tanh[f(z,t)]\right)+\left(B^2+2A\right)\tanh^2[f(z,t)]\right)}{S(B+K\tanh[f(z,t)])^2}, \tag{55}$$

where k_1, E, A, B, N, c are non-zero real constants, and $S = 1+B^2Nk_1^2-4NAk_1^2$, $H = 2Nk_1^2\left(B^2-4A\right)$, $K = \sqrt{B^2-4A}$, $f(z,t) = \frac{K}{2}\left(k_1z-\frac{k_1c}{\sqrt{1+B^2Nk_1^2-4NAk_1^2}}t+E\right)$.

$$U_5(z,t) = \frac{\left(H\left(-B^2+6A+2iKB\tan[g(z,t)]\right)+\left(B^2+2A\right)\tan^2[g(z,t)]\right)}{S(-B+iK\tan[g(z,t)])^2}, \tag{56}$$

where k_1, E, A, B, N, c are non-zero real constants, and $S = 1+B^2Nk_1^2-4NAk_1^2$, $H = 2Nk_1^2\left(B^2-4A\right)$, $K = \sqrt{B^2-4A}$, $g(z,t) = \frac{iK}{2}\left(k_1z-\frac{k_1c}{\sqrt{1+B^2Nk_1^2-4NAk_1^2}}t+E\right)$.

$$U_6(z,t) = -\frac{2\,N\,k_1^2(B^2+2\,A)}{S} + \frac{12B^3N\,k_1^2\left(k_1z-\frac{k_1c}{\sqrt{S}}t+E\right)}{S\left(2B\left(k_1z-\frac{k_1c}{\sqrt{S}}t+E\right)+4\right)} - \frac{12B^4N\,k_1^2\left(k_1z-\frac{k_1r}{\sqrt{S}}t+E\right)^2}{S\left(2B\left(k_1z-\frac{k_1c}{\sqrt{S}}t+E\right)+4\right)^2}. \tag{57}$$

where k_1, E, A, B, N, c are non-zero real constants, and $S = 1+B^2Nk_1^2-4NAk_1^2$.

Thirdly, we calculate the hyperbolic, trigonometric, rational and exponential functions solutions for Equation (1) by substituting the coefficient values from Equation (49) into Equation (46) and considering Equations (34)–(36) as follows:

$$U_7(z,t) = -2+\frac{2k_2^2}{c^2k_1^2}+\frac{12A\,N^2k_2^2\left(c^2k_1^2-k_2^2\right)\,\mathrm{sec}\,h^2(\beta_3\,(k_1z+k_2t+E))}{c^2\left(\alpha_1-\sqrt{N\left(c^2k_1^2-k_2^2\right)}\tanh\left(\beta_3\,(k_1z+k_2t+E)\right)\right)^2}, \tag{58}$$

where k_1, k_2, E, A, N, c are non-zero real constants, and $\alpha_1 = \sqrt{N\left(4NAk_1^2k_2^2-c^2k_1^2+k_2^2\right)}$, $\beta_3 = \frac{1}{2}\sqrt{\frac{c^2k_1^2-k_2^2}{Nk_1^2k_2^2}}$.

$$U_8(z,t) = -2+\frac{2k_2^2}{c^2k_1^2}+\frac{12A\,N^2k_2^2\left(c^2k_1^2-k_2^2\right)\,\mathrm{sec}^2(\beta_4\,(k_1z+k_2t+E))}{c^2\left(\alpha_1+\sqrt{N\left(k_2^2-c^2k_1^2\right)}\tan\left(\beta_4\,(k_1z+k_2t+E)\right)\right)^2}, \tag{59}$$

where k_1, k_2, E, A, N, c are non-zero real constants, and $\alpha_1 = \sqrt{N\left(4NAk_1^2k_2^2+c^2k_1^2-k_2^2\right)}$, $\beta_4 = \frac{1}{2}\sqrt{\frac{k_2^2-c^2k_1^2}{Nk_1^2k_2^2}}$.

$$U_9(z,t) = -2+\frac{2k_2^2}{c^2k_1^2}+\frac{3\,N\left(-16\alpha_1k_1k_2+\alpha_1^2(k_1z+k_2t+E)\right)}{c^2k_1^2(\alpha_1(k_1z+k_2t+E)-2Nk_1k_2)^2}, \tag{60}$$

where k_1, k_2, E, A, N, c are non-zero real constants, and $\alpha_1 = \sqrt{N\left(4NAk_1^2k_2^2+c^2k_1^2-k_2^2\right)}$.

Fourthly, we calculate the hyperbolic, trigonometric, rational and exponential functions solutions for Equation (28) by substituting the coefficient values from Equation (50) into Equation (46) and considering Equations (34)–(36) as follows:

$$U_{10}(z,t) = -\frac{9Na_0\left(k_2^2-c^2k_1^2\right)}{c^2\left(\delta\,\cosh(\beta_1(k_1z+k_2t+E))+3\sqrt{N\left(k_2^2-c^2k_1^2\right)}\sinh(\beta_1(k_1z+k_2t+E))\right)^2}, \tag{61}$$

where k_1, k_2, E, a_0, N, c are non-zero real constants, and $\delta = \sqrt{-3N\left(c^2a_0k_1^2+3c^2k_1^2-3k_2^2\right)}$, $\beta_1 = \frac{1}{2}\sqrt{\frac{k_2^2-c^2k_1^2}{Nk_1^2k_2^2}}$.

$$U_{11}(z,t) = \frac{9Na_0\left(c^2k_1^2-k_2^2\right)\,\mathrm{sec}^2(\beta_3(k_1z+k_2t+E))}{c^2\left(\delta\,-3\sqrt{N\left(c^2k_1^2-k_2^2\right)}\tan(\beta_3(k_1z+k_2t+E))\right)^2}, \tag{62}$$

where k_1, k_2, E, a_0, N, c are non-zero real constants, and $\delta = \sqrt{-N\left(c^2a_0k_1^2+3c^2k_1^2-3k_2^2\right)}$, $\beta_3 = \frac{1}{2}\sqrt{\frac{c^2k_1^2-k_2^2}{Nk_1^2k_2^2}}$.

$$U_{12}(z,t) = \frac{9N\left(-4\sqrt{3}k_1k_2\omega_1\left(c^2k_1^2-k_2^2\right)(k_1z+k_2t+E)+c^2k_1^4\left(4Nk_2^2+a_0\right)-\omega_2(k_1z+k_2t+E)^2\right)}{c^2k_1^2\left(\sqrt{3}\omega_1(k_1z+k_2t+E)+6Nk_1k_2\right)^2}, \tag{63}$$

where k_1, k_2, E, a_0, N, c are non-zero real constants, and $\omega_1 = \sqrt{-N\left(r^2(a_0+3)k_1^2-3k_2^2\right)}$, $\omega_2 = \left(c^2k_1^2k_2^2(a_0+6)\,-3k_2^4-c^4k_1^4(a_0+3)\right)$.

Lastly, we calculate the hyperbolic, trigonometric, rational, and exponential functions solutions for Equation (28) by substituting the coefficient values from Equation (51) into Equation (46) and considering Equations (34)–(36) as follows:

$$U_{13}(z,t) = -\frac{3\left(c^2k_1^2-k_2^2\right)\left(q-3c^2k_1^2a_0\tanh^2(\beta_3(k_1z+k_2t+E))+4ip\sqrt{c^2k_1^2-k_2^2}\tanh(\beta_3(k_1z+k_2t+E))\right)}{c^2k_1^2\left(ip+\sqrt{c^2k_1^2-k_2^2}\tanh(\beta_3(k_1z+k_2t+E))\right)^2}, \quad (64)$$

where k_1, k_2, E, a_0, N, c are non-zero real constants, and $p = \sqrt{3\left(c^2a_0k_1^2-c^2k_1^2+k_2^2\right)}$, $q = c^2a_0k_1^2+8c^2k_1^2-8k_2^2$, $\beta_3 = \frac{1}{2}\sqrt{\frac{c^2k_1^2-k_2^2}{Nk_1^2k_2^2}}$.

$$U_{14}(z,t) = \frac{3N\left(c^2k_1^2-k_2^2\right)\left(-q-3c^2k_1^2a_0\tan^2(\beta_1(k_1z+k_2t+E))+4ip\sqrt{k_2^2-c^2k_1^2}\tan(\beta_1(k_1z+k_2t+E))\right)}{c^2k_1^2N\left(ip+\sqrt{k_2^2-c^2k_1^2}\tan(\beta_1(k_1z+k_2t+E))\right)^2}, \quad (65)$$

where k_1, k_2, E, a_0, N, c are non-zero real constants, and $p = \sqrt{3\left(c^2a_0k_1^2-c^2k_1^2+k_2^2\right)}$, $q = c^2a_0k_1^2+8c^2k_1^2-8k_2^2$, $\beta_1 = \frac{1}{2}\sqrt{\frac{k_2^2-c^2k_1^2}{Nk_1^2k_2^2}}$.

$$U_{15}(z,t) = a_0 + \frac{Np^2(k_1z+k_2t+E)\left(-i4\sqrt{N}pk_1k_2+p^2(k_1z+k_2t+E)\right)}{c^2k_1^2N\left(6Nk_1k_2-ip\sqrt{N}(k_1z+k_2t+E)\right)^2}, \quad (66)$$

where k_1, k_2, E, a_0, N, c are non-zero real constants, and $p = \sqrt{3\left(c^2a_0k_1^2-c^2k_1^2+k_2^2\right)}$.

6. Results and Discussion

In this section, the generalized exp $(-\phi(\eta))$ expansion function method was developed and has been utilized in solving the longitudinal wave equation in a magneto-electro-elastic circular rod, and various solutions in hyperbolic function, trigonometric function, periodic solitary wave, rational function, bright and dark solitons solutions, sinh, cosh, and sech^2 function solutions form were obtained. These soliton solutions can help to explain the dynamics of higher-order dispersion, full nonlinearity, and spatiotemporal dispersion. They can also be utilized to the propagation of solitons through a variety of waveguides. The nonlinear DNA lattice, long–short-wave interaction systems, double-strand dynamics in biophysics, ultrashort pulses in metamaterials, blood flow in arteries, solitons in periodic resonant media, coupled waveguide arrays in nonlinear optics, and seismic sea waves are just a few examples of physical challenges that have been modeled using solitary waves. We plotted some of the solutions to have an idea on the mechanism of the original Equation (28). We examined the nature of numerous solutions to the model of MEE circular rod as non-linear dynamics of radially displaced by selecting certain parameter values and plotting the precise solutions produced by the use of the mathematical software Mathematica 10. We specifically plotted solutions Equations (52)–(66) using appropriate values of the obtained parameters. The graphs of these solutions are presented in Figures 2–16, respectively. We discovered that some of the solutions in this study possess significant physical meanings, such as the hyperbolic tangent, which appears in the calculation of magnetic moment and special relativity rapidity.

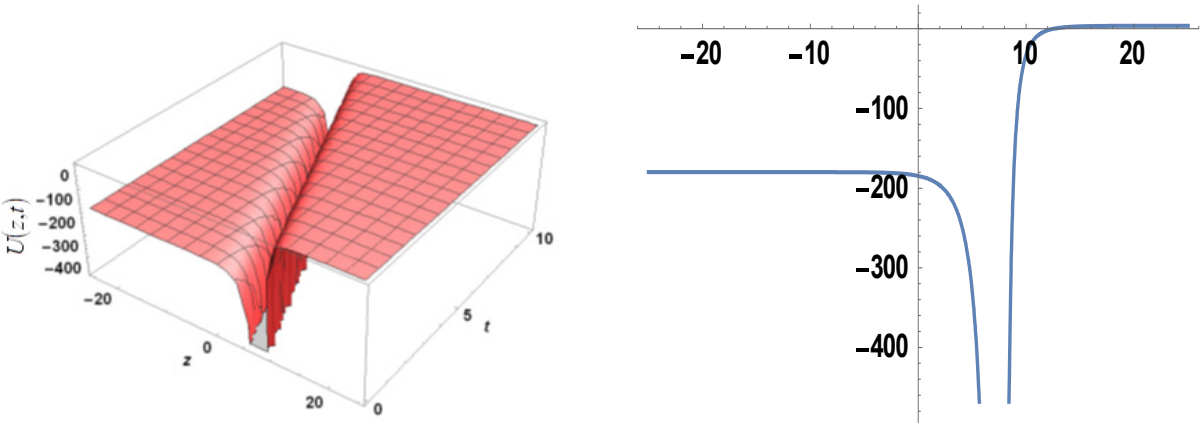

Figure 2. The 3D and 2D plots of Equation (52) for various values of parameters.

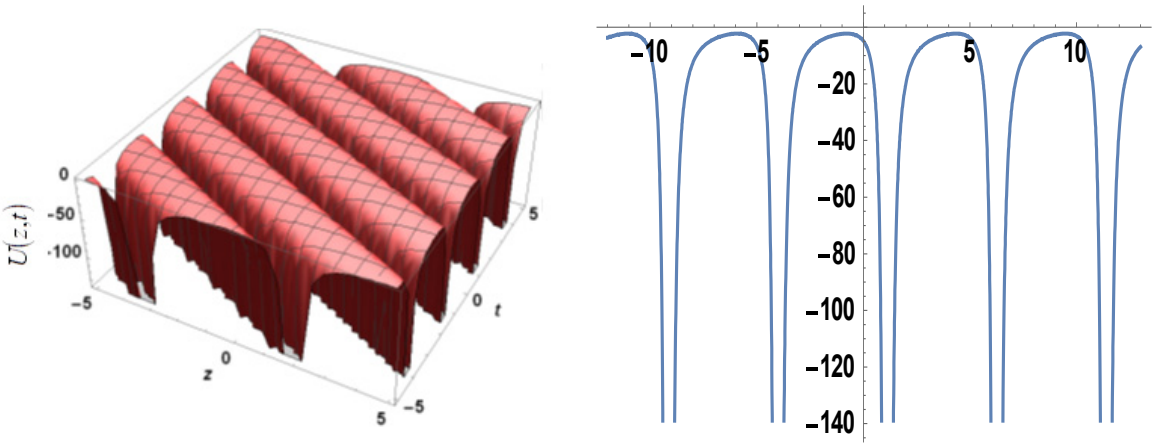

Figure 3. The 3D and 2D plots of Equation (53) for various values of parameters.

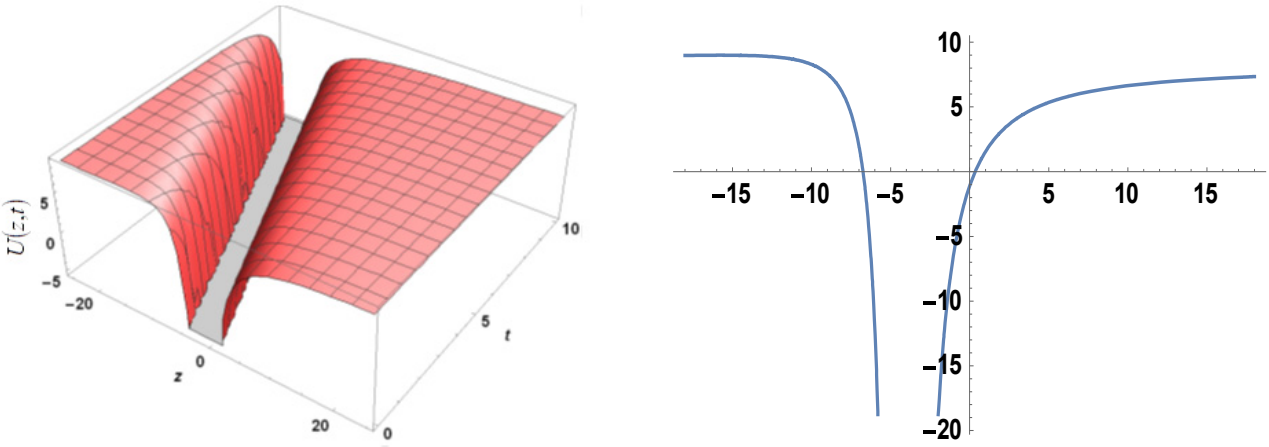

Figure 4. The 3D and 2D plots of Equation (54) for various values of parameters.

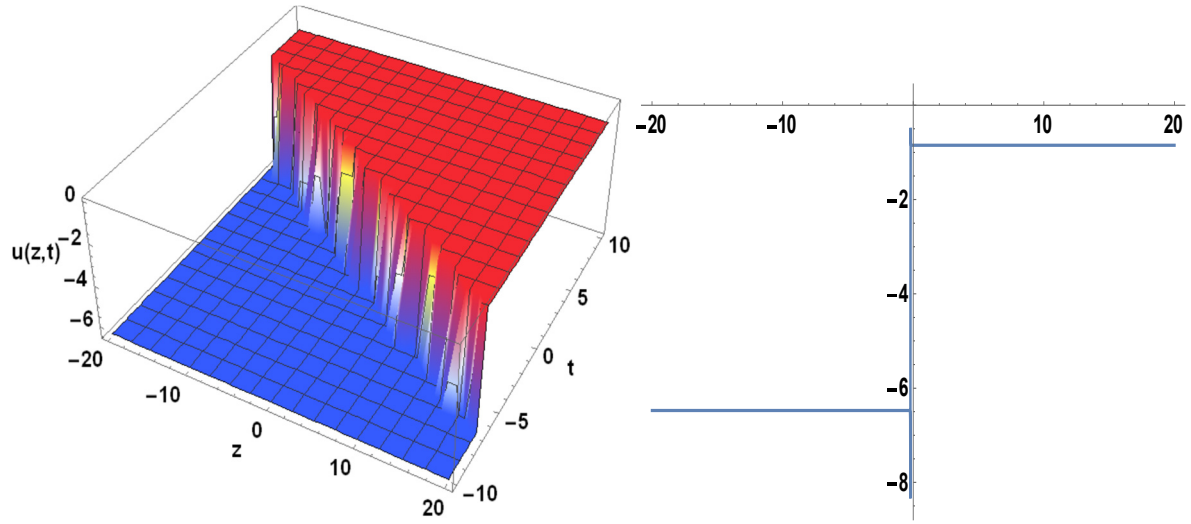

Figure 5. The 3D and 2D plots of Equation (55) for various values of parameters.

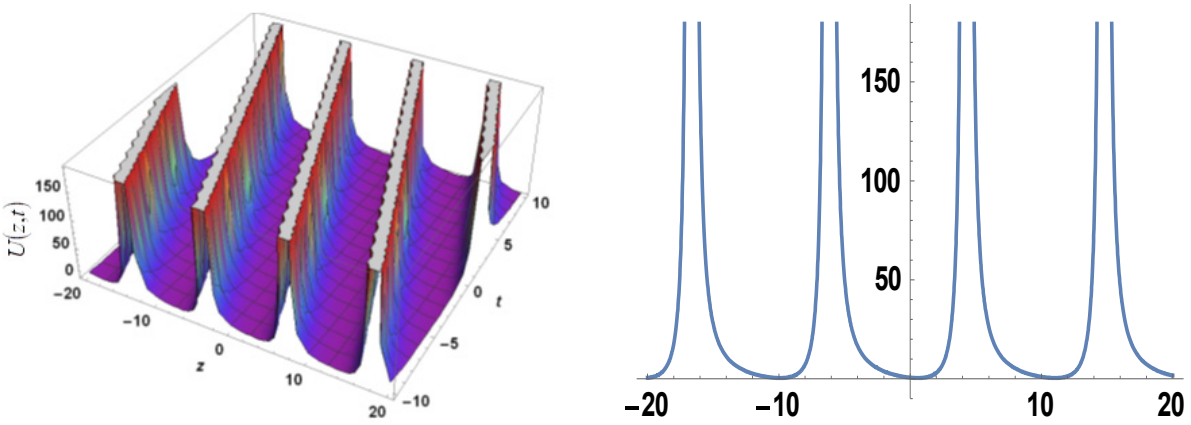

Figure 6. The 3D and 2D plots of Equation (56) for various values of parameters.

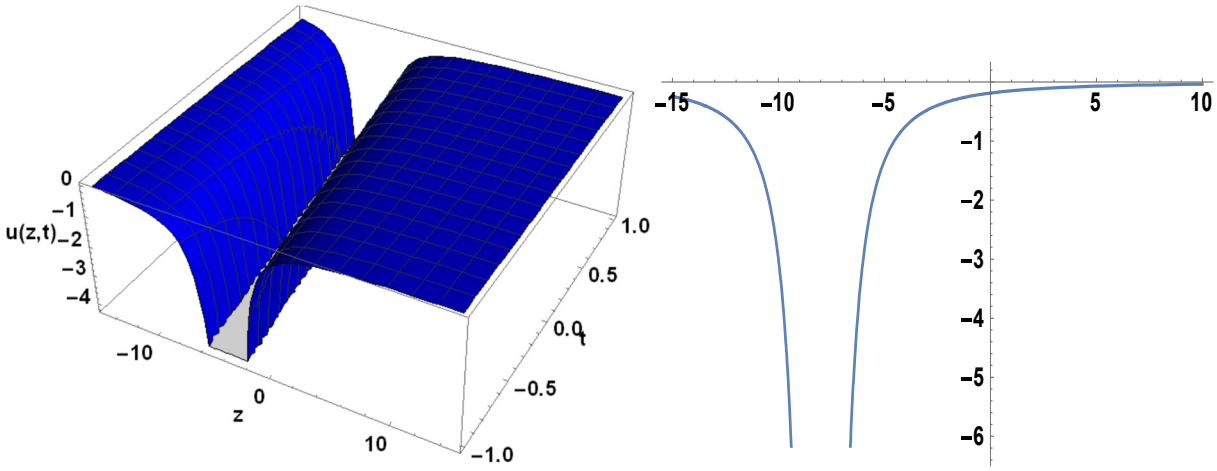

Figure 7. The 3D and 2D plots of Equation (57) for various values of parameters.

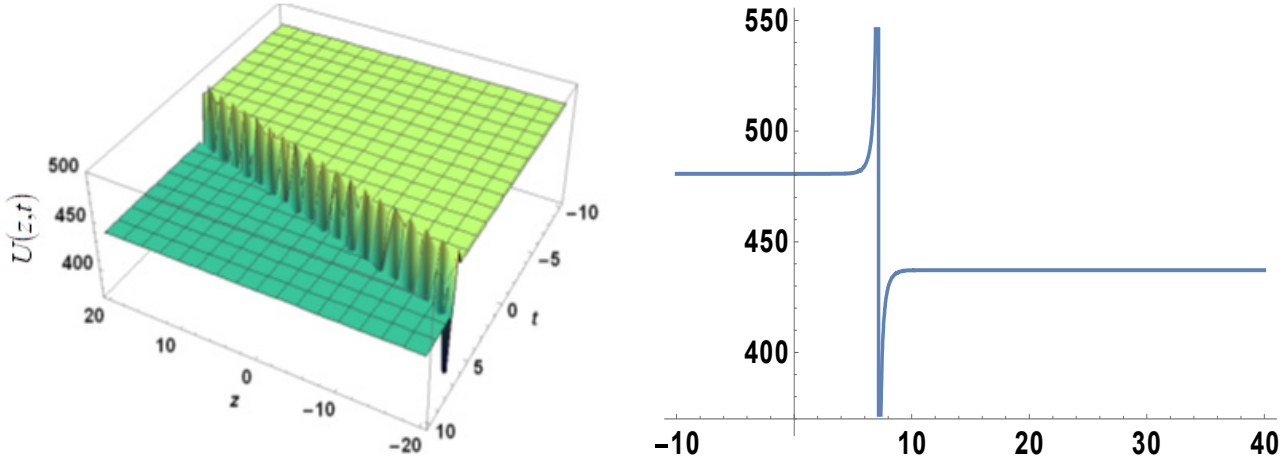

Figure 8. The 3D and 2D plots of Equation (58) for various values of parameters.

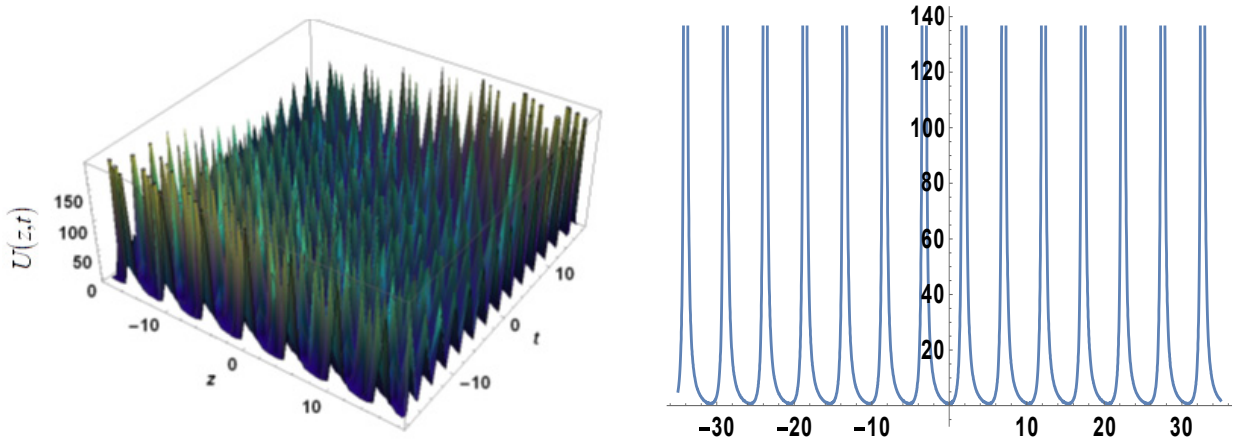

Figure 9. The 3D and 2D plots of Equation (59) for various values of parameters.

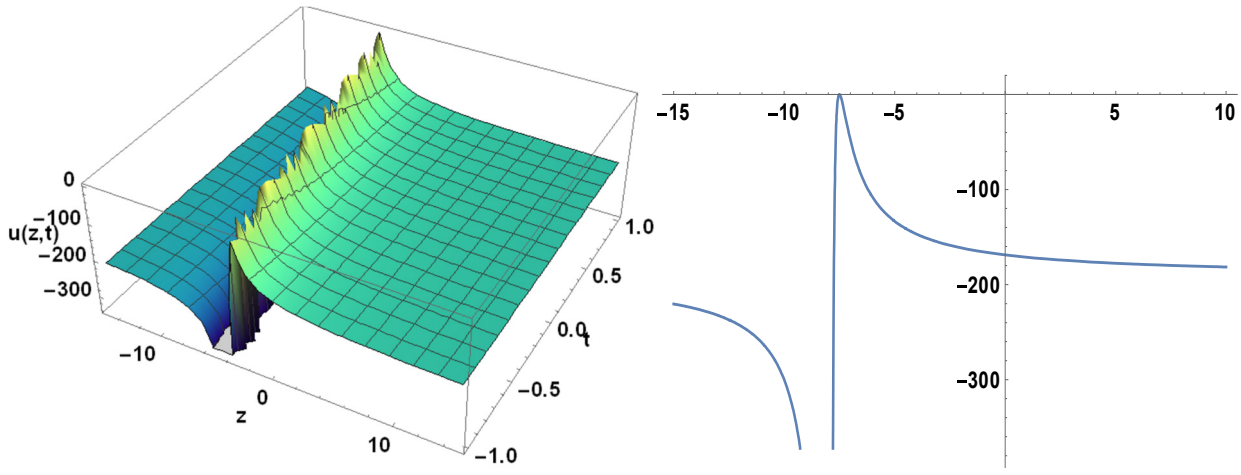

Figure 10. The 3D and 2D plots of Equation (60) for various values of parameters.

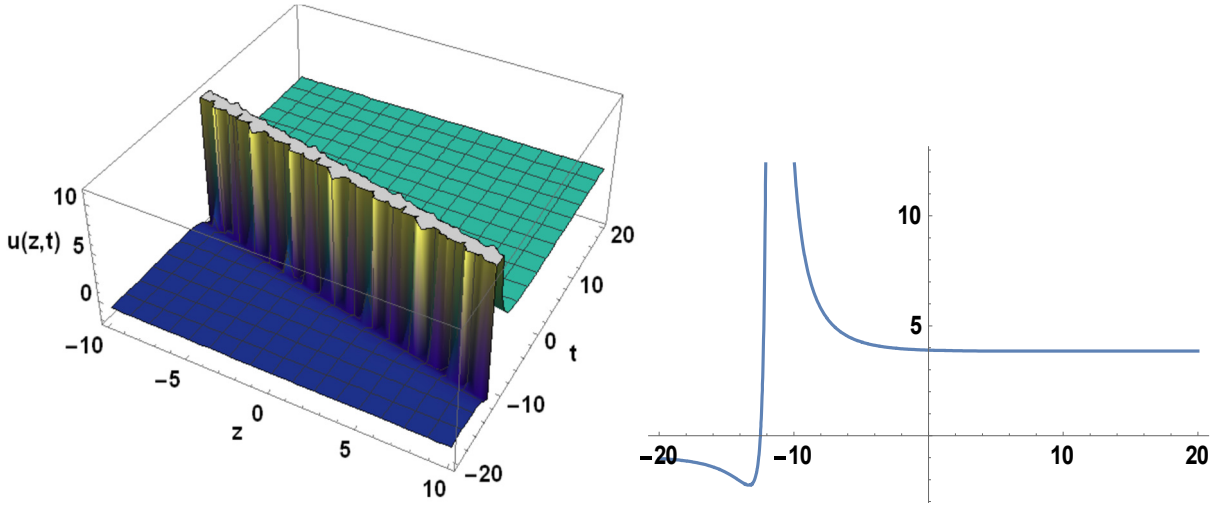

Figure 11. The 3D and 2D plots of Equation (61) for various values of parameters.

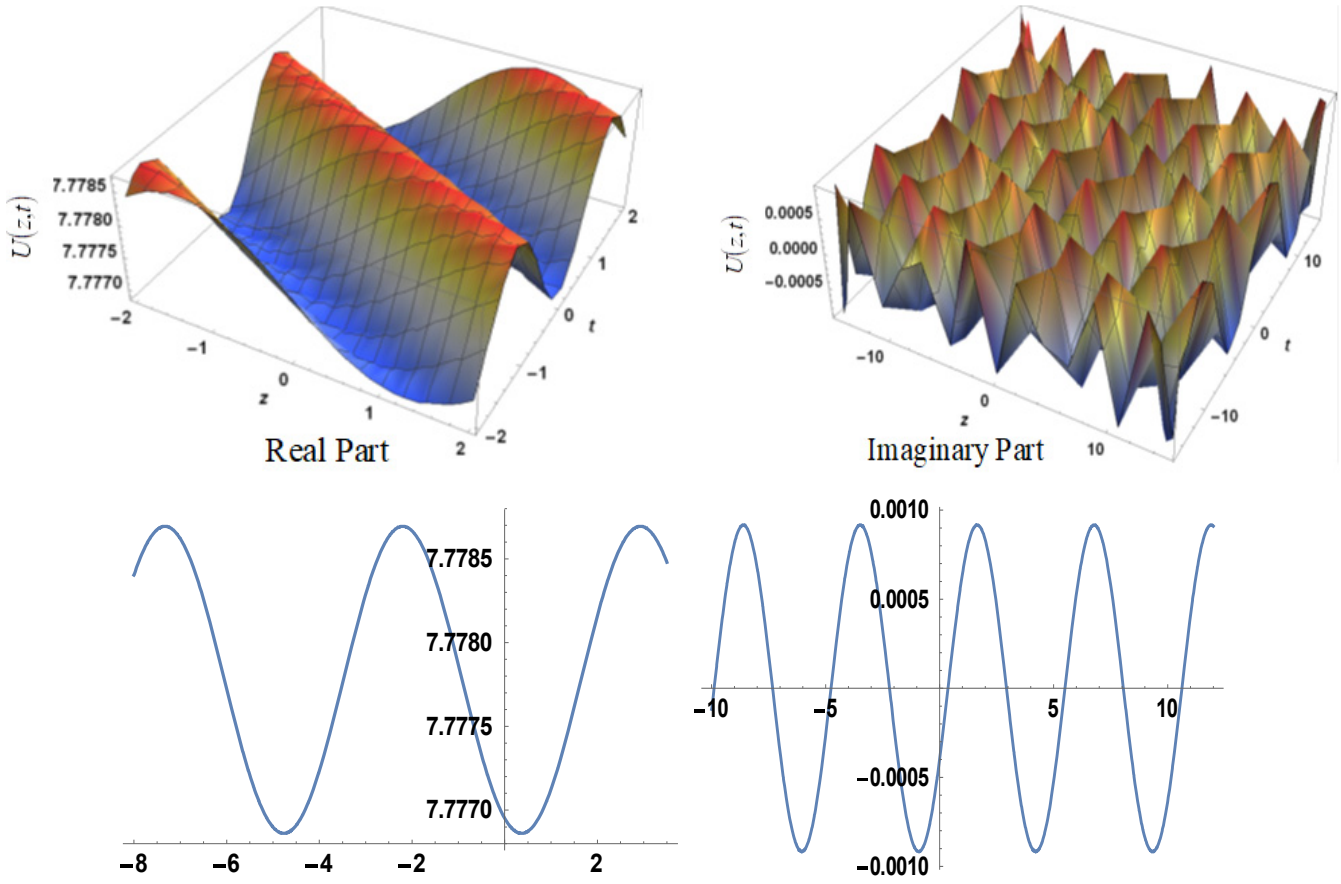

Figure 12. The 3D and 2D plots of Equation (62) for various values of parameters.

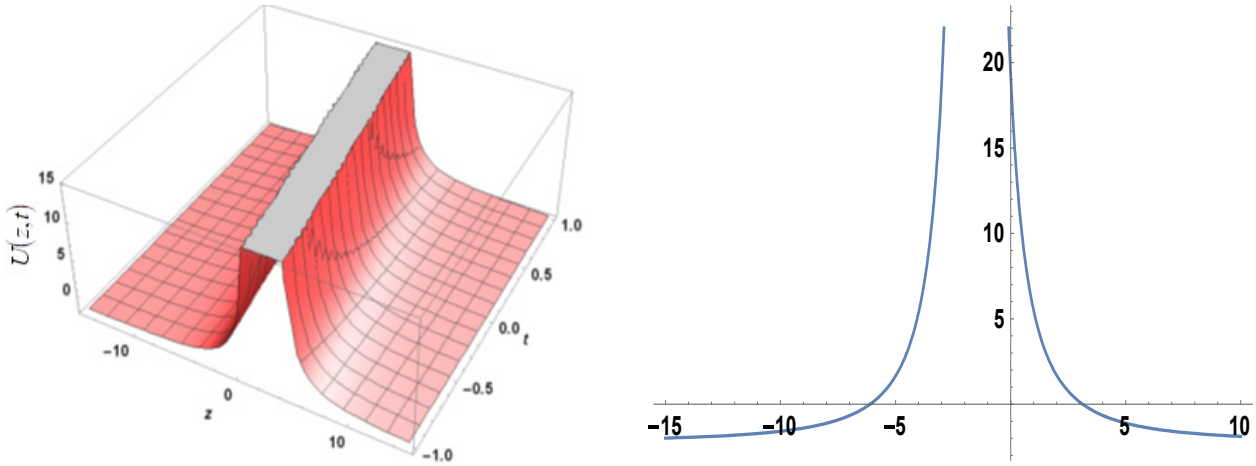

Figure 13. The 3D and 2D plots of Equation (63) for various values of parameters.

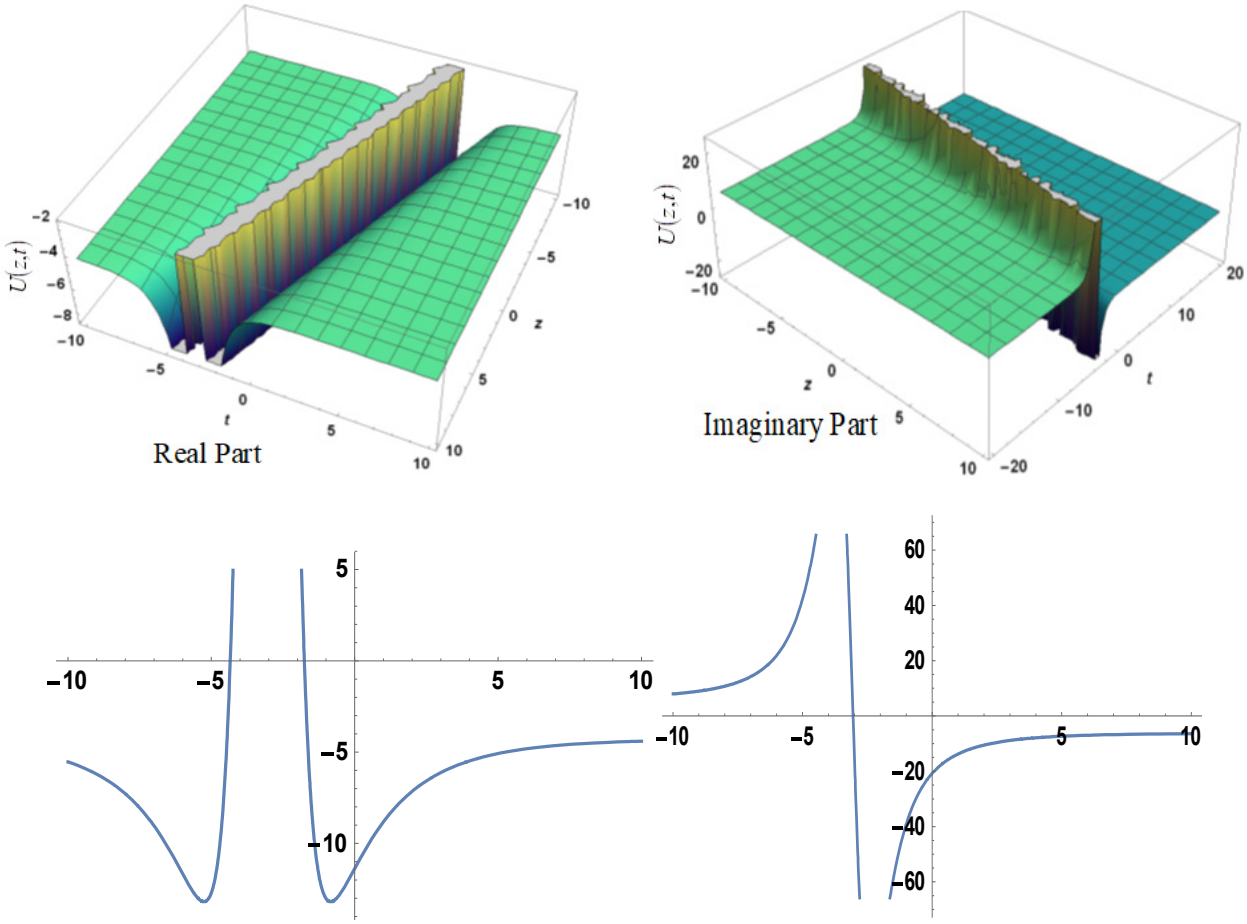

Figure 14. The 3D and 2D plots of Equation (64) for various values of parameters.

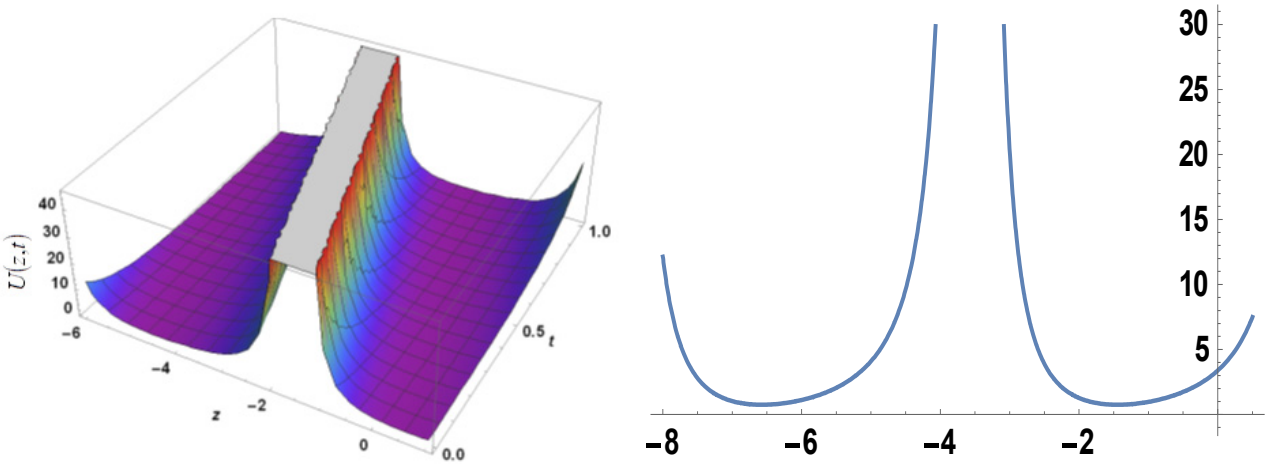

Figure 15. The 3D and 2D plots of Equation (65) for various values of parameters.

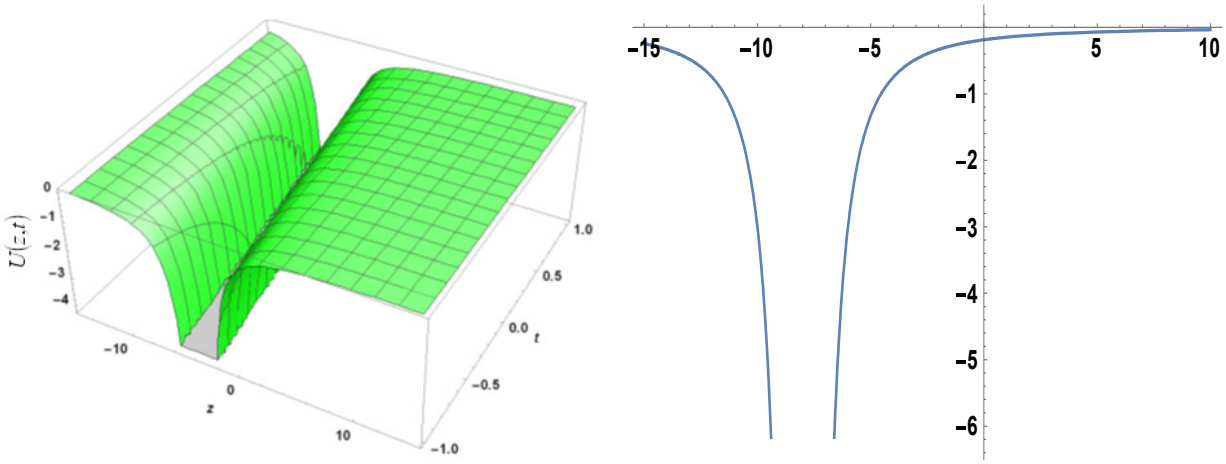

Figure 16. The 3D and 2D plots of Equation (66) for various values of parameters.

Graphical representations are a highly helpful tool for communicating and clearly and succinctly describing problem solutions. A graph is an easily compared visual representation of quantitative or qualitative solutions or other facts. We wish to have a fundamental understanding of the graphs when performing computations. A hyperbolic function solution is represented by Equation (52). Singular kink solutions are waves that travel from one asymptotic state to the next. At infinity, the singular kink solutions approach a constant. Figure 2 pageants the shape of singular soliton exact solution for 3D and 2D plots of $U_1(z, t)$ for the unknown constants $k_1 = 0.5$, $k_2 = 1$, $c = 1$, $N = 2$, $A = 1$, and $E = 0.1$ within the interval $-25 \leq z \leq 25$, $0 \leq t \leq 10$ for the 3D graph and $t = 0.01$ for the 2D graph. Equation (53) represents the exact periodic travelling wave solution. The 3D and 2D plots for $U_2(z, t)$ are shown in Figure 3 for unknown parameters $k_1 = 0.5$, $k_2 = 1$, $c = -4$, $N = 2$, $A = 2$, and $E = 0.1$ and within the interval $-5 \leq x, t \leq 5$ for the 3D graph and $t = 0.5$ for 2D graph. Figure 4 represents the 3D and 2D plots for dark singular soliton wave solution of $U_3(z, t)$ for parameters $k_1 = 0.5$, $k_2 = 1$, $c = 1$, $N = 2$, $A = 1$, and $E = 0.1$ and within the interval $-5 \leq z \leq 5$, $-2 \leq t \leq 2$ for the 3D graph and $t = 1$ for the 2D graph. Figure 5 displays the 3D and 2D plots for kink-type solution of $U_4(z, t)$ for $k_1 = 15$, $c = 4$, $N = 2$, $B = 13$, $A = 12$, and $E = 5$ and within the interval $-20 \leq z \leq 20$, $-10 \leq t \leq 10$ for the 3D graph and $t = 0.01$ for the 2D graph. The trigonometric function solution in Figure 6 demonstrates the periodic soliton solutions of $U_5(z, t)$ for the unknown constants $k_1 = 0.3$, $c = 3$, $N = -2$, $B = 3$, $A = 2$, and $E = 5$ to the interval $-20 \leq z \leq 20$, $-10 \leq t \leq 10$ for the 3D graph and $t = 10$ for 2D graph. The 3D plot to the rational function solution $U_6(z, t)$ in Equation (57) that behaves like a singular soliton solution for the unknown constants $k_1 = 0.3$,

$c = 3$, $N = -2$, $B = 3$, $A = 2$, and $E = 5$, and within the interval $-15 \leq z \leq 15, -1 \leq t \leq 1$ for 3D graphs and $t = 1$ for 2D graphs is shown in Figure 7. The hyperbolic function solution in Figure 8 demonstrates the singular kink-type wave solutions of $U_7(z, t)$ for the unknown constants $k_1 = 0.1$, $k_2 = 0.6$, $c = 0.4$, $N = -0.2$, $A = 2$, and $E = 0.1$ in the interval $-20 \leq z \leq 20$, $-10 \leq t \leq 10$ for the 3D graph and $t = 1$ for 2D graph. Figure 9 represents the 3D and 2D new periodic soliton solution to the Equation (60) for different values of the parameters $k_1 = 0.5$, $k_2 = 1$, $c = 4$, $N = -2$, $A = 2$, and $E = 1$ and to the interval $-18 \leq z, t \leq 18$ for the 3D graph and $t = 30$ for the 2D graph. Figure 10 shows the singular kink-type soliton solution for $U_9(z, t)$ for unknown constants $k_1 = 1$, $k_2 = 2$, $c = 2$, $N = 4$, $A = 1$, and $E = 5$ for 3D graph within the interval $-15 \leq z \leq 15$, $-1 \leq t \leq 1$ and $t = 1$ for 2D graph. Figure 11 represents bright singular solitons trajectory of $U_{10}(z, t)$ for the known parameters $k_1 = 0.3$, $k_2 = 0.6$, $a_0 = 1$, $c = 4$, $N = 2$, and $E = 1$ for 3D graph and $t = 0.1$ for the 2D graph within the intervals $-10 \leq z \leq 10$, $-20 \leq t \leq 20$. The real and imaginary parts of $U_{11}(z, t)$ in Figure 12 show the breaking soliton and periodic solutions for various values of the parameters $k_1 = 0.5$, $k_2 = 1$, $a_0 = -10$, $c = 4$, $N = 2$, and $E = 0.1$ for 3D and $t = 0.1$ for 2D plots. Figure 13 shows the singular soliton solution for the unknown constants $k_1 = 0.3$, $k_2 = 0.6$, $\alpha_0 = 1$, $c = 4$, $N = -16$, and $E = 1$ for 3D graphs within the interval $-15 \leq z \leq 15$, $-1 \leq t \leq 1$ and $t = 1$ for 2D graphs. Figure 14 shows the real and imaginary parts of hyperbolic function solution of $U_{13}(z, t)$ for the unknown constant $k_1 = 2$, $k_2 = 6$, $a_0 = 2$, $c = 4$, $N = 5$, and $E = 0.1$ for 3D graphs within the interval $-10 \leq z, t \leq 10$, and $t = 1$ for 2D graphs, which shows multiple bright singular soliton solution. Figure 15 represents the 3D and 2D plots of the trigonometric function solution $U_{14}(z, t)$, which shows periodic solution for the unknown constants $k_1 = 0.5$, $k_2 = 1$, $a_0 = 1$, $c = -4$, $N = -2$, and $E = 0.1$ for 3D graphs within the interval $-6 \leq z \leq 1$, $0 \leq t \leq 1$ and $t = 1$ for 2D graphs. Figure 16 shows the singular soliton solution for the unknown constants $k_1 = 0.3$, $k_2 = 0.6$, $a_0 = 1$, $c = 4$, $N = -16$, and $E = 1$ for 3D graphs within the interval $-15 \leq z \leq 15$, $-1 \leq t \leq 1$ and $t = 1$ for 2D graphs.

7. Conclusions

In the current study, we investigated the generalized exp $(-\phi(\eta))$ expansion approach to identify various types of new precise travelling and solitary wave solutions of one-dimensional nonlinear LWE in a circular MEE rod. This effective approach can also be used to resolve a wide variety of nonlinear evolution equations that arise in the fields of engineering, plasma, hydrodynamics, mathematical physics, and other applied sciences. As a result, we were able to acquire several single-wave electrostatic potential and pressure solutions, demonstrating the efficiency and dependability of this technique. The solitary wave solutions are acquired in the form of bright and dark solitons, sinh and cosh function solutions, sech^2 function solutions, periodic solitary wave, rational function, and complex hyperbolic function solutions. There are numerous mathematical and mathematical physics applications that involve the hyperbolic functions. For instance, the gravitational potential of a cylinder gives birth to the hyperbolic sine. The shape of a dangling cable can be seen in the hyperbolic cosine function. The computation and speed of special relativity give rise to the hyperbolic tangent. All three can be seen in general relativity's Schwarzschild metric when employing external isotropic Kruskal coordinates. The hyperbolic secant appears in a laminar jet's profile. The Langevin function for magnetic polarization contains the hyperbolic cotangent. The analytical results from Section 5 are connected to the physical characteristics of hyperbolic functions. Particularly, it is projected that the complex hyperbolic function solutions U_{13} discovered in this study will represent the gravitational potential of a cylinder described by Equation (28). They are also displayed in two- and three-dimensional graphs. This can also aid researchers in their understanding of an investigation into the system's scientific explanation. Many existing solutions in the literature were re-derived when parameters were given specific values, demonstrating the novelty of our work. Similarly, if we use Equations (37)–(43), we obtain numerous new and interesting

solutions. This method can be used to obtain not only exponential function solutions but also hyperbolic, trigonometric, and rational function solutions. The generalized exp $(-\phi(\eta))$ expansion method has been demonstrated to be an effective method for obtaining closed-form solutions to other nonlinear partial differential equations.

Author Contributions: Data curation, W.W.; Funding acquisition, W.W.; Methodology, A.; Software, M.K.A.; Validation, A.M.Z.; Writing—original draft, M.S.; Writing—review & editing, N.A.S. All authors have read and agreed to the published version of the manuscript.

Funding: This work received no external funding.

Data Availability Statement: No data were used to support this study.

Acknowledgments: The authors extends their appreciation to the Deanship of Scientific Research at King Khalid University, Abha 61413, Saudi Arabia, for funding this work through a research group program under grant number R.G.P.-2/65/43. This research received funding support from the NSRF via the Program Management Unit for Human Resources & Institutional Development, Research and Innovation, (grant number B05F650018).

Conflicts of Interest: The authors declare no conflict of interest.

References

1. Benjamin, T.B. The stability of solitary waves. *Proc. R. Soc. A* **1972**, *328*, 153–183.
2. Xue, C.X.; Pan, E.; Zhang, S.Y. Solitary waves in a magneto-electro-elastic circular rod. *Smart Mater. Struct.* **2011**, *20*, 105010. [CrossRef]
3. Kozhekin, A.; Kurizki, G. Self-induced transparency in Bragg reflectors: Gap solitons near absorption resonances. *Phys. Rev. Lett.* **1995**, *74*, 5020. [CrossRef]
4. Vlasov, R.A.; Lemeza, A.M. Bistable moving optical solitons in resonant photonic crystals. *Phys. Rev. A* **2011**, *84*, 023828. [CrossRef]
5. Russell, J.S. *Report on Waves: Made to the Meetings of the British Association in 1842-43*; John Murray: London, UK, 1845; pp. 311–390.
6. Chen, J.Y.; Pan, E.; Chen, H.L. Wave propagation in magneto-electro-elastic multilayered plates. *Int. J. Solids Struct.* **2007**, *44*, 1073–1085. [CrossRef]
7. Chen, P.; Shen, Y. Propagation of axial shear magneto–electro-elastic waves in piezoelectric–piezomagnetic composites with randomly distributed cylindrical inhomogeneities. *Int. J. Solids Struct.* **2007**, *44*, 1511–1532. [CrossRef]
8. Wu, B.; Yu, J.G.; He, C.F. Wave propagation in non-homogeneous magneto-electro-elastic plates. *J. Sound Vib.* **2008**, *317*, 250–264.
9. Seadawy, A.R. Nonlinear wave solutions of the three-dimensional Zakharov–Kuznetsov–Burgers equation in dusty plasma. *Phys. A Stat. Mech. Its Appl.* **2015**, *439*, 124–131. [CrossRef]
10. Seadawy, A.R. Travelling-wave solutions of a weakly nonlinear two-dimensional higher-order Kadomtsev-Petviashvili dynamical equation for dispersive shallow-water waves. *Eur. Phys. J. Plus* **2017**, *132*, 1–13. [CrossRef]
11. Abdullah; Seadawy, A.R.; Jun, W. Mathematical methods and solitary wave solutions of three-dimensional Zakharov-Kuznetsov-Burgers equation in dusty plasma and its applications. *Results Phys.* **2017**, *7*, 4269–4277. [CrossRef]
12. Chen, Y.; Yan, Z.; Zhang, H. Exact Solutions for a Family of Variable-Coefficient "Reaction–Duffing" Equations via the Bäcklund Transformation. *Theor. Math. Phys.* **2002**, *132*, 970–975. [CrossRef]
13. Manafian, J.; Lakestani, M. Optical solitons with Biswas-Milovic equation for Kerr law nonlinearity. *Eur. Phys. J. Plus* **2015**, *130*, 61. [CrossRef]
14. Kourakis, I.; Moslem, W.M.; Abdelsalam, U.M.; Sabry, R.; Shukla, P.K. Nonlinear dynamics of rotating multi-component pair plasmas and epi plasmas. *Plasma Fusion Res.* **2009**, *4*, 018. [CrossRef]
15. Seadawy, A.R. Modulation instability analysis for the generalized derivative higher order nonlinear Schrödinger equation and it's the bright and dark soliton solutions. *J. Electromagn. Waves Appl.* **2017**, *31*, 1353–1362. [CrossRef]
16. Seadawy, A.R.; El-Rashidy, K. Traveling wave solutions for some coupled nonlinear evolution equations. *Math. Comput. Model.* **2013**, *57*, 1371–1379. [CrossRef]
17. Seadawy, A.R. Exact solutions of a two-dimensional nonlinear Schrödinger equation. *Appl. Math. Lett.* **2012**, *25*, 687–691. [CrossRef]
18. Manafian, J.; Lakestani, M. Solitary wave and periodic wave solutions for Burgers, Fisher, Huxley and combined forms of these equations by the (G′/G)-expansion method. *Pramana* **2015**, *85*, 31–52. [CrossRef]
19. Teymuri, S.C.; Manafian, J. Wave solutions for variants of the KdV–Burger and the K (n, n)–Burger equations by the generalized G′/G-expansion method. *Math. Methods Appl. Sci.* **2017**, *40*, 4350–4363. [CrossRef]
20. Helal, M.A.; Seadawy, A.R.; Zekry, M.H. Stability analysis of solitary wave solutions for the fourth-order nonlinear Boussinesq water wave equation. *Appl. Math. Comput.* **2014**, *232*, 1094–1103. [CrossRef]

21. He, W.; Chen, N.; Dassios, I.; Shah, N.A.; Chung, J.D. Fractional system of Korteweg-De Vries equations via Elzaki transform. *Mathematics* **2021**, *9*, 673. [CrossRef]
22. Shah, N.A.; Agarwal, P.; Chung, J.D.; El-Zahar, E.R.; Hamed, Y.S. Analysis of optical solitons for nonlinear Schrödinger equation with detuning term by iterative transform method. *Symmetry* **2020**, *12*, 1850. [CrossRef]
23. Shah, N.A.; Alyousef, H.A.; El-Tantawy, S.A.; Shah, R.; Chung, J.D. Analytical investigation of fractional-order Korteweg–De-Vries-type equations under Atangana–Baleanu–Caputo operator: Modeling nonlinear waves in a plasma and fluid. *Symmetry* **2022**, *14*, 739. [CrossRef]
24. Seadawy, A.R.; Lu, D.; Khater, M.M.A. Bifurcations of solitary wave solutions for the three dimensional Zakharov–Kuznetsov–Burgers equation and Boussinesq equation with dual dispersion. *Optik* **2017**, *143*, 104–114. [CrossRef]
25. Lu, D.; Seadawy, A.R.; Arshad, M.; Wang, J. New solitary wave solutions of (3+ 1)-dimensional nonlinear extended Zakharov-Kuznetsov and modified KdV-Zakharov-Kuznetsov equations and their applications. *Results Phys.* **2017**, *7*, 899–909. [CrossRef]
26. Arshad, M.; Seadawy, A.R.; Lu, D. Exact bright–dark solitary wave solutions of the higher-order cubic–quintic nonlinear Schrödinger equation and its stability. *Optik* **2017**, *138*, 40–49. [CrossRef]
27. Ghany, H.A. Exact solutions for stochastic fractional Zakharov-Kuznetsov equations. *Chin. J. Phys.* **2013**, *51*, 875–881.
28. Arshad, M.; Seadawy, A.R.; Lu, D.; Wang, J. Travelling wave solutions of Drinfel'd–Sokolov–Wilson, Whitham–Broer–Kaup and (2+ 1)-dimensional Broer–Kaup–Kupershmit equations and their applications. *Chin. J. Phys.* **2017**, *55*, 780–797. [CrossRef]
29. Ali, A.; Seadawy, A.R.; Lu, D. Soliton solutions of the nonlinear Schrödinger equation with the dual power law nonlinearity and resonant nonlinear Schrödinger equation and their modulation instability analysis. *Optik* **2017**, *145*, 79–88. [CrossRef]
30. Seadawy, A.R. The generalized nonlinear higher order of KdV equations from the higher order nonlinear Schrödinger equation and its solutions. *Optik* **2017**, *139*, 31–43. [CrossRef]
31. Rani, A.; Shakeel, M.; Kbiri Alaoui, M.; Zidan, A.M.; Shah, N.A.; Junsawang, P. Application of the $\mathrm{Exp}(-\varphi(\xi))$ −Expansion Method to Find the Soliton Solutions in Biomembranes and Nerves. *Mathematics* **2022**, *10*, 3372. [CrossRef]
32. Ali, A.; Seadawy, A.R.; Lu, D. Computational methods and traveling wave solutions for the fourth-order nonlinear Ablowitz-Kaup-Newell-Segur water wave dynamical equation via two methods and its applications. *Open Phys.* **2018**, *16*, 219–226. [CrossRef]
33. Shang, Y. Lie algebraic discussion for affinity based information diffusion in social networks. *Open Phys.* **2017**, *15*, 705–711. [CrossRef]
34. Shang, Y. Analytical solution for an in-host viral infection model with time-inhomogeneous rates. *Acta Phys. Pol. B* **2015**, *46*, 1567–1577. [CrossRef]
35. Shang, Y. A lie algebra approach to susceptible-infected-susceptible epidemics. *Electron. J. Differ. Eq.* **2012**, *2012*, 1–7.
36. Shakeel, M.; Attaullah; El-Zahar, E.R.; Shah, N.A.; Chung, J.D. Generalized Exp-Function Method to Find Closed Form Solutions of Nonlinear Dispersive Modified Benjamin–Bona–Mahony Equation Defined by Seismic Sea Waves. *Mathematics* **2022**, *10*, 1026. [CrossRef]
37. Yahya, K.H.; Moussa, Z.A. New approach of generalized exp $(-\phi(\xi))$ expansion method and its application to some nonlinear partial differential equation. *J. Math. Res.* **2015**, *7*, 106–121.
38. Baskonus, H.M.; Bulut, H.; Atangana, A. On the complex and hyperbolic structures of the longitudinal wave equation in a magneto-electro-elastic circular rod. *Smart Mater. Struct.* **2016**, *25*, 035022. [CrossRef]
39. Younis, M.; Ali, S. Bright, dark, and singular solitons in magneto-electro-elastic circular rod. *Waves Random Complex Media* **2015**, *25*, 549–555. [CrossRef]
40. Ma, X.; Pan, Y.; Chang, L. Explicit travelling wave solutions in a magneto-electro-elastic circular rod. *Int. J. Comput. Sci. Issues* **2013**, *10*, 62.
41. Khan, K.; Koppelaar, H.; Akbar, M.A. Exact and numerical soliton solutions to nonlinear wave equations. *Casp. J. Comput. Math. Eng.* **2016**, *2*, 5–22.
42. Seadawy, A.R.; Manafian, J. New soliton solution to the longitudinal wave equation in a magneto-electro-elastic circular rod. *Results Phys.* **2018**, *8*, 1158–1167. [CrossRef]